Uncovering circadian rhythm disruptions of synaptic proteome signaling in prefrontal cortex and nucleus accumbens associated with opioid use disorder

Stephanie Puig[1,2], Xiangning Xue[3], Ryan Salisbury[2], Micah A. Shelton[2], Sam-Moon Kim[2], Mariah A. Hildebrand[2], Jill R. Glausier[2], Zachary Freyberg[2,3], George C. Tseng[4], Anastasia K. Yocum[5], David A. Lewis[2], Marianne L. Seney[2], Matthew L. MacDonald[2*], and Ryan W. Logan[2,6,7,8*]

[1]Department of Pharmacology, Physiology and Biophysics, Boston University School of Medicine, Boston, MA, USA

[2]Department of Psychiatry, University of Pittsburgh School of Medicine, Pittsburgh, PA, USA

[3]Department of Cell Biology, University of Pittsburgh, Pittsburgh, PA, USA

[4]Department of Biostatistics, University of Pittsburgh, Pittsburgh, PA, USA

[5]A2IDEA, Inc., Ann Arbor, MI, USA

[6]Department of Psychiatry, University of Massachusetts Chan Medical School, Worcester, MA, USA

[7]Department of Neurobiology, University of Massachusetts Chan Medical School, Worcester, MA, USA

[8]Morningside Graduate School of Biomedical Sciences, University of Massachusetts Chan Medical School, Worcester, MA, USA

***Co-corresponding authors**
Ryan W. Logan, PhD
364 Plantation Street, LRB Office 611
Worcester, MA 01605
ryan.logan@umassmed.edu

Matthew L. MacDonald
203 Lothrop St,
Thomas E. Starzl Biomedical Science Tower, Room W1655
Pittsburgh, PA 15213
macdonaldml@upmc.edu

Abstract

Opioid craving and the vulnerability to relapse is associated with severe and persistent disruptions to sleep and circadian rhythms. Investigations into the cellular and molecular pathways in the human brain underlying the relationship between circadian rhythms and OUD remain limited. In human subjects with OUD, previous transcriptomics work implicated a role for circadian regulation of synaptic processes in key cognitive- and reward-related brain regions, dorsolateral prefrontal cortex (DLPFC) and nucleus accumbens (NAc). To provide further insights into the synaptic alterations associated with OUD, we used mass-spectrometry based proteomics to deeply profile protein alterations in tissue homogenates and synaptosomes from both NAc and DLPFC of unaffected and OUD subjects. Between unaffected and OUD subjects, we identified 43 differentially expressed (DE) proteins in NAc homogenates and 55 DE proteins in DLPFC homogenates. In synaptosomes, we found 56 DE proteins in NAc of OUD subjects and 161 DE proteins in DLPFC. Examining synaptosome enrichment of specific proteins enabled us to identify brain region- and synapse-specific pathway alterations in NAc and DLPFC associated with OUD. Across both regions, we found OUD-associated protein alterations primarily in pathways involved in GABAergic and glutamatergic synaptic functions, as well as circadian rhythms. Using time-of-death (TOD) analyses, where the TOD of each subject is used as a time-point across a 24-hour cycle, we were able to map circadian-related changes in the synaptic proteomes in NAc and DLPFC associated with OUD. In OUD, TOD analysis revealed significant circadian changes in endoplasmic reticulum to Golgi vesicle-mediated transport and protein membrane trafficking in NAc synapses, accompanied by changes in platelet derived growth factor receptor beta

signaling in DLPFC synapses. Together, our results lend further support for molecular disruption of circadian regulation of synaptic signaling in the human brain as a key factor in opioid addiction.

Introduction

Rates of opioid use disorder (OUD) and deaths from opioid overdoses have continued to rise over the recent decade from 2012-2022 in the United States [1]. Understanding the impact of long-term opioid use and overdose on the human brain is critical for developing new interventions, therapeutics, and for evaluating current OUD treatments. In-depth investigations into the cellular and molecular changes in human postmortem brain may provide valuable insights into the biological mechanisms associated with OUD and lead to new therapeutic strategies for treating opioid addiction [2–8].

The dorsolateral prefrontal cortex (DLPFC) and nucleus accumbens (NAc) are key brain regions involved in cognitive, mood, and reward alterations in OUD [9–11]. Recent human postmortem brain studies from us [2, 3] and others [4, 6, 12, 13] reported a potential interplay between proinflammatory and synaptic remodeling in DLPFC and NAc in OUD. Moreover, we recently implicated circadian rhythm regulation of neuroinflammatory, neurovascular, and neurotransmission (*e.g.,* dopaminergic, GABAergic, and opioidergic signaling) in DLPFC and NAc of OUD subjects [2, 3]. Transcriptional rhythm alterations in both brain regions were linked to sleep and circadian rhythm traits in OUD [2], further supporting mechanistic relationships between sleep and circadian disruption in synaptic changes in opioid addiction [2, 14–22]

To date, much of the work in postmortem human brain of subjects with OUD has used RNA-sequencing approaches, with few proteomics studies [13]. Transcriptomics and proteomics approaches provide different levels of biological information. Transcriptomics on bulk tissue homogenates from postmortem brain mostly provides

molecular information on the cell bodies, with limited insight into function, especially synaptic processes. Complementary to transcriptomics, proteomics reports on the cell bodies and neuropils, (including synapses and glial processes). Advances in proteomic approaches are capable of deeply profiling the peptides in synaptosomes from human brain and their changes associated with psychiatric disorders [23]. Therefore, proteomics approaches in tissue homogenates and synaptosomes from human brain may reveal functional changes in specific cell types and synapses associated with OUD.

Using quantitative mass spectrometry (MS) using tandem mass tags (TMT) [24, 25], we deeply profiled both tissue homogenates and synaptosomes isolated from postmortem NAc and DLPFC of unaffected comparison subjects and subjects with OUD. Our approach enabled the identification of proteins preferentially enriched in specific synaptic subtypes. Overall, we found changes associated with OUD in protein pathways related to neuroinflammation and neurodegeneration across both NAc and DLPFC. Further, we discovered significant alterations in GABAergic and glutamatergic synaptic processes across brain regions in OUD subjects. Notably, these synaptic changes were also associated with disruptions to circadian rhythm signaling in NAc and DLPFC. Using time-of-death (TOD) analysis, we captured OUD-associated circadian rhythm alterations of protein expression in synaptosomes. At the synaptic level, circadian disruption was connected with alterations in endoplasmic reticulum, protein trafficking, and platelet derived growth factor (PDGF) signaling dysfunction in OUD, in addition to significant changes in GABAergic and glutamatergic synaptic functions. Together, our results indicated putative roles for protein pathways involved in neurodegeneration, inhibitory and

excitatory neurotransmission in OUD, and implicated circadian regulation of opioid-induced synaptic alterations in opioid addiction.

Materials and Methods

Human Subjects

Following consent from next-of-kin, postmortem brains were obtained during autopsies at Allegheny County (Pittsburgh, PA, USA; N=39) or Davidson Country (Nashville, TN, USA; N=1) Medical Examiner's Office. An independent committee of clinicians made consensus, lifetime DSM-IV diagnoses for each subject based on results from psychological autopsy, including structured family interviews, medical record reviews, and toxicological and neuropathological reports [26]. Similar procedures were used to confirm absence of lifetime psychiatric and neurological disorders in unaffected subjects. Procedures were approved by University of Pittsburgh Committee for Oversight of Research and Clinical Training Involving Decedents and Institutional Review Board for Biomedical Research. Each subject with OUD was matched with an unaffected comparison subject for sex and age [2, 3]. Cohorts differed by race ($p=0.02$) and brain pH ($p=0.015$, 0.2 pH units mean difference), and did not significantly differ in postmortem interval (PMI), RNA integrity number (RIN), or TOD ($p>0.25$; Supplementary Table S1). TOD was determined from the death investigation report (Medical Examiner's Office). DLPFC and NAc were anatomically identified and collected, as previously described [2, 3].

Brain Sample Preparation for Mass Spectrometry

Gray matter tissue (~20mg) from DLPFC (area 9) and NAc were collected from fresh-frozen coronal tissue blocks via cryostat, using an approach to minimize contamination from white matter and other subregions [27, 28]. Homogenate and

synaptosome preparations were obtained using a variation of our enrichment protocol for postmortem human brain tissues [23, 29, 30] with SynPER reagent (ThermoFisher). From each sample, 10µg total protein (as measured by Micro BCA) was reduced, alkylated, and trypsin digested on S-Trap™ micro spin columns (ProtiFi). Subject pairs were randomly assigned to TMT blocks and labeled with TMTPro channels 1-10, with brain regions and preparations assigned to separate blocks [31]. Additional aliquots from each sample were used for a pooled control, digested separately with S-Trap Midi™ columns, divided then labeled with TMTPro channels 1 and 12. TMT labeled preparations from the same block were pooled with 10µg of the labeled pooled controls. The TMT labeled peptide pools were separated into eight fractions with the Pierce™ High pH Reversed-Phase Peptide Fractionation Kit (ThermoFisher Scientific), evaporated, and reconstituted in 20 µl 97% H2O, 3% ACN, 0.1% formic acid.

Mass Spectrometry

TMT labeled peptides (~1µg) were loaded onto a heated PepMap RSLC C18 column (2 µm, 100 angstrom, 75 µm × 50 cm; ThermoScientific), then eluted over 180 min gradients optimized for each high pH reverse-phase fraction [25]. Sample eluate was electrosprayed (2000 V) into an Orbitrap Eclipse Mass Spectrometer (MS; ThermoFisher Scientific) for analysis. MS1 spectra were acquired at a resolving power of 120,000. MS2 spectra were acquired in the Ion Trap with CID (35%) in centroid mode. Real-time search (RTS) (max search time = 34 s; max missed cleavages = 1; Xcorr = 1; dCn = 0.1; ppm = 5) was used to select ions for SPS for MS3. MS3 spectra were acquired in the Orbitrap with

HCD (60%) with an isolation window = 0.7m/z and a resolving power of 60,000, and a max injection time of 400ms.

Data Processing

Raw MS files were processed in Proteome Discoverer (v. 2.5; ThermoFisher Scientific). MS spectra were searched against the *Homo sapiens* SwissProt database. SEQUEST search engine was used (enzyme=trypsin, maximum missed cleavage=2, minimum peptide length=6, precursor tolerance=10ppm). Static modifications include acetylation (N-term, +42.011 Da), Met-loss (N-term, -131.040 Da), Met-loss+Acetyl (N-temr, -89.030 Da), and TMT labeling (N-term and K, +229.163 Da). Dynamic modification, oxidation (M, +15.995 Da). PSMs were filtered by the Percolator node (maximum Delta Cn=0.05, FDR =0.01). Reporter ion quantification was based on intensity values with the following settings/filters: integration tolerance=20ppm, method=most confident centroid, co-isolation threshold=100, and SPS mass matches [%] threshold = 65. Peptide intensity values were normalized within and across TMT plexes with Normalization Mode=Total Peptide Amount and Scaling Mode=On All Average in Proteome Discoverer. Peptides used to sum to protein measures were determined using “Unique + Razor”. Only proteins of high confidence were retained for statistical analyses and protein values were log2 transformed prior to analysis. The mass spectrometry proteomics data have been deposited to the ProteomeXchange Consortium via the PRIDE partner repository [32] with the dataset identifier PXD041333 and 10.6019/PXD041333.

Differential Expression of Proteins

Limma-Voom with covariate selection (covariates included TMT plex, sex, age, PMI, and peptide expression) was used to detect differentially expressed (DE) proteins between unaffected subjects and subjects with OUD in homogenate and synaptosome protein fractions for each brain region [23]. Proteins were considered DE if both $p<0.05$ and $\log_2$ fold-change (logFC) were greater than or equal to ±0.26 (20% change in protein expression), as previously used [3, 33, 34]. Over-representation pathway analyses were completed using clusterProfiler [35] and ReactomePA [36] for DE proteins in homogenates and synaptosomes. For pathway enrichments in DE proteins, the range of gene set size was 10-500 with a q-value cutoff of 0.1 and adjusted p-value by Benhamini-Hochberg of 0.05. Rank-rank hypergeometric (RRHO) was used to detect overlap of altered proteins between unaffected and OUD subjects across brain regions. Synaptic and homogenate protein levels were compared to determine protein enrichments in synaptosomes. Within unaffected and OUD subjects, the abundance of each protein identified in synaptosomal preparations was compared to the abundance of that protein in the total tissue homogenate preparation. Proteins with significantly greater levels of expression in synaptosomal preparations (Bonferroni-corrected $p<0.05$) and showed a difference of at least 1.25-fold in the synaptosome relative to homogenate were classified as synaptically-enriched proteins. All other proteins, by default, were defined as non-enriched. Statistical analysis of synaptosome differences between unaffected and OUD subjects were limited to these enriched synaptic proteins, as described previously [23].

Diurnal Rhythmicity

For each subject, TOD was converted to Zeitgeber Time (ZT) by using the times of sunrise and sunset on the day of death (ZT0 is sunrise, negative ZTs reflect hours prior to sunrise). Sinusoidal curves were fitted using nonlinear least-squares regression with the coefficient of determination used as a proxy of goodness-of-fit (R^2). Estimates of empirical p-values were determined using null distributions of R^2 generated from 1,000 TOD-randomized expression datasets. Diurnal rhythms of protein expression in homogenates and synaptosomes were first identified separately in unaffected subjects and subjects with OUD. Rhythmic proteins were then compared between unaffected and OUD subjects ($p<0.05$; Fisher's exact test). A complementary analysis determined which proteins exhibited a significant change in rhythmicity between unaffected comparison and OUD subjects ($\Delta R^2 = R^2$ Unaffected - R^2 OUD). This change in rhythmicity analysis was restricted to proteins that were significantly rhythmic in unaffected or OUD subjects. Proteins were identified as significantly less rhythmic in OUD versus unaffected subjects if $\Delta R^2 > 0$ or more rhythmic if $\Delta R^2 < 0$. Null distributions of ΔR^2 were permuted 1,000 times, whereby the unaffected and OUD subjects were permuted independently to generate null distributions (R^2 unaffected and R^2 OUD). Significantly less or more rhythmic in OUD was calculated by comparing the ΔR^2 to the null ΔR^2 for unaffected and OUD subjects. Differences in phase, amplitude, and base (mesor of fitted curve) were also calculated and restricted to significantly rhythmic proteins from both unaffected and OUD subjects. Pathway enrichments were completed by Metascape (Gene Ontology; Hallmark; Reactome; Canonical; metascape.org) [37] for protein rhythm analyses.

Heatmaps represent protein expression rhythms for the top rhythmic proteins in homogenates and synaptosomes for each brain region. Protein expression was Z-

transformed and ordered by phase (ZT of peak expression). Each column represents a subject, ordered by ZT. Heatmaps were generated for 1) top 200 rhythmic proteins in unaffected subjects; 2) top 200 rhythmic proteins identified in unaffected subjects then plotted for OUD subjects to assess alterations in circadian proteomes in OUD; 3) top rhythmic proteins in OUD subjects; 4) top 200 rhythmic proteins in OUD subjects then plotted for unaffected subjects.

Weighted Gene Co-Expression Network Analysis

To identify co-expression protein modules, we used weighted gene co-expression network analysis (WGCNA) on protein expression from homogenates or synaptosomes within each brain region and group [2, 3, 38–40]. Module differential connectivity (MDC) analyses examined the impact of OUD on protein co-expression network modules. For each module, the degree of connection was calculated in both unaffected and OUD subjects. MDC was defined as the ratio of the protein co-expression connections between unaffected and OUD subjects. To assess significance of MDC, we permuted (1000 times) the samples and module members to generate null distribution. When a module was built on unaffected subjects, a significant MDC greater than 1 indicated a gain of connectivity of the modules in OUD, while a significant MDC less than 1 indicated a loss of connectivity. Modules were tested for enrichment of DE proteins and rhythmic proteins in unaffected and OUD. ARACne was used to identify hub proteins in each module [41]. Proteins with an adjacency value higher than the 90th quantile were considered neighbors. Hub proteins were identified with the highest number of N-hob neighborhood nodes (NHNN) than the average. Hub proteins specific to unaffected and OUD subjects were

considered disease-specific hub proteins. Hub gene networks were plotted using Cytoscape (3.9.1). We then identified enriched pathways of synaptic specific protein co-expression networks using SynGo [42].

Results

Brain Region-specific Protein Alterations in Tissue Homogenates and Synaptosomes associated with OUD in NAc and DLPFC

We investigated differences in protein expression in tissue homogenates from both DLPFC and NAc of subjects with OUD compared to unaffected subjects. We identified 43 DE ($p<0.05$ and logFC±0.26) proteins (14 upregulated and 29 downregulated; Fig. 1a, Supplementary Tables S2, S3) in the NAc of subjects with OUD. In DLPFC,we identified 55 DE proteins, with a majority being upregulated in OUD (46 upregulated and 9 downregulated; Fig. 1b, Supplementary Tables S4, S5). We also isolated synaptosomes for high-density protein profiling in both NAc and DLPFC from unaffected and OUD subjects. In synaptosomes, we found 56 DE proteins (17 upregulated and 39 downregulated) in NAc (Fig. 1e, Supplementary Table S7, S8) and 161 DE proteins (80 upregulated and 81 downregulated) in DLPFC (Fig. 1f, Supplementary Table S9, S10).

To investigate the possible similarities of protein alterations between brain regions, we compared protein changes between NAc and DLPFC in OUD subjects using the threshold-free approach, RRHO [58, 59]. Overall, we found weak concordance between NAc and DLPFC of upregulated and downregulated proteins in OUD subjects (Fig. 1c), despite identifying overlapping proteins between these brain regions (Fig. 1d). In contrast, we previously reported remarkable concordance between NAc and DLPFC in both upregulated and downregulated transcripts associated with OUD of the same subjects investigated here [2, 3]. In synaptosomes, we identified no significant overlap of protein changes between brain regions (Fig. 1g,h). Therefore, protein alterations were unique between brain regions in OUD, and together with our previous results [2], may reflect

complex brain region-specific, post-transcriptional and translational mechanisms impacted by opioids.

Enrichment of Protein Pathways involved in Immune Modulation and Neurodegeneration in NAc and DLPFC Tissue Homogenates associated with OUD

To further define the biological significance of the protein alterations in OUD, we conducted pathway enrichment analysis on DE proteins from tissue homogenates of NAc and DLPFC (Fig. 2, Supplementary Table S6). In NAc homogenates, enrichment analyses identified pathways related to immune modulatory pathways, including various types of infection (*e.g.,* KRT14,16,17 [43]; HLA-B [44]) leukocyte migration (*e.g.,* JAM2 [45]; PLCG1 [46]). Notably, neurodegeneration pathways were also enriched in NAc homogenates (Fig. 2a; *e.g.,* CHRM1 [47, 48]; MAPT [49]; SQSTM1 [50]). Similarly, several pathways related to neurodegeneration were highly enriched in DLPFC homogenates from subjects with OUD, such as Alzheimer (43 proteins; *e.g.,* SLC25A6 [51]; CHRM3 [52]; MTOR [53]; ITPR2 [54]), Huntington (38 proteins; *e.g.,* PSMD11 [55]; ADRM1 [56]; SOD1 [57]), Parkinson (41 proteins; PARK7 [58]; HTRA2 [59]), and prion (42 proteins; *e.g.,* RYR2 [60]) disease-related pathways (Fig. 2b). Other pathways specifically enriched in DLPFC homogenates were pathways related to cell stress including oxidative phosphorylation and reactive oxygen species (Fig. 2b). Together, our findings in tissue homogenates highlight a possible cascade of immune activation and diminished cellular health associated with OUD in human brain.

Differential Enrichment between Tissue Homogenates and Synaptosomes Highlights a Altered GABAergic and Glutamatergic Synaptic Signaling in NAc and DLPFC associated with OUD

We aimed to reveal protein expression changes between unaffected and OUD subjects preferential to synaptosomes. To identify synaptically enriched proteins, we compared the relative expression of each protein between homogenates and synaptosomes within each brain region, followed by differential expression between unaffected and OUD cohorts. We identified proteins primarily expressed and altered in tissue homogenates of OUD subjects and proteins preferentially expressed in synaptosomes (Supplementary Tables S7-S12). Our approach enabled us to examine pathways with specific enrichments in synaptosomes unique and common to each brain region. Synaptosomes from NAc were enriched for several pathways involved in mitochondrial and endoplasmic reticulum functions (proximal tubule bicarbonate reclamation, carbohydrate digestion and absorption), along with second messenger signaling cascades (cGMP-PKG and cAMP: *e.g.,* GNAI2,3; GABRA2; ACY1; Fig. 2a, Supplementary Table S6). Other pathways were specifically enriched in synaptosomes of DLPFC from OUD subjects, such as ribosome, relaxin, and Rap1 signaling (Fig. 2b). OUD-related alterations in serotonergic synapses (*e.g.,* GNAO1; GNAS; GNAI2,3, GNB1,4) were also unique to DLPFC (Fig. 2b, Supplementary Table S6).

Additionally, we found pathways that were similarly altered across brain regions in synaptosomes. The major pathways enriched across NAc and DLPFC synaptosomes included morphine addiction, along with GABAergic (*e.g.,* GNG3, GABBR2, GNB1 in

NAc; and GNAO1, GNB4, SLC6A11 in DLPFC) and glutamatergic synapses (*e.g.,* GNG3, SLC1A3, and ADCY1 in NAc; and GNAO1, GNAS, and GNB14 in DLPFC; Fig. 2a,b).

Further investigation of the individual proteins enriched in synaptosomes revealed THY1 [61, 62], CACNA2D1 [63–66], SLC3A2 [67], GSK3B [68–70], LSAMP [71, 72], LY6H [73, 74], and NCAM1 [75–79], as the top synaptic proteins altered in NAc of OUD subjects (Fig. 3). In DLPFC, proteins altered in OUD and enriched in synaptosomes included RALB [80], CADM3 [81, 82], GPC1 [83], MRAS, CNTFR [84], IGLON5 [85], IST1, and PLXNA4 [86, 87] (Fig. 3). Other synaptically-enriched proteins in DLPFC were similar to those enriched in NAc (*e.g.,* GSK3B, LSAMP, NCAM1, CACNA2D1, SLC3A2; Fig. 3). Consistent with our pathway enrichments in synaptosomes of OUD subjects (Fig. 2), many of the synaptically enriched proteins across NAc and DLPFC are involved in GABAergic and glutamatergic synaptic functions. For example, CACNA2D1, SLC3A2, and GSK3B dynamically regulate the activity of glutamatergic-dependent synaptic activity and plasticity [66, 67, 69].

Pathway Enrichment Reveal Role for Circadian Rhythms in Synaptic Alterations associated with OUD

We previously reported transcriptional rhythm disruptions in both NAc and DLPFC in subjects with OUD [2]. In support of this, circadian entrainment was a significantly enriched pathway in synaptosomes from NAc and DLPFC of OUD subjects (Fig. 2). Several proteins that were enriched specifically in synaptosomes have integral roles in the regulation of circadian rhythms (*e.g.,* CACNA2D1, GSK3B, NCAM1, SYT3 [88]; Fig. 3). To further explore circadian rhythms in brain proteomes, we conducted TOD analysis

on homogenate (Supplementary Fig. S2, Supplementary Tables S13-20) and synaptosomal (Fig. 4) proteins in each brain region. In NAc homogenates of OUD subjects, top enriched pathways included opioid and synaptic signaling (Supplementary Fig. S2). DARRP32, a phosphoprotein critically involved in dopaminergic synaptic functions, was among the top rhythmic proteins in OUD (Supplementary Fig. S2). Rhythmic proteins specifically in NAc of OUD subjects were associated with pathways in various vesicle endocytotic processes (*e.g.,* endocytosis, synaptic vesicle cycle, and clathrin-mediated endocytosis; Supplementary Fig. S2). In DLPFC, top rhythmic proteins in OUD subjects included the neurosecretory protein, VGF [89], and the putative negative regulator of cannabinoid receptor 1 activity, CNRIP1[168] (Supplementary Fig. S2). Top rhythmic pathways in OUD were related to glial cell development, mitochondrion organization, and various components of lipid and pyruvate metabolism (Supplementary Fig. S2). Our previous work reported disrupted transcriptional rhythms in NAc and DLPFC of the same OUD subjects investigated here [2]. Rhythmicity in transcript abundance was more prevalent compared to rhythms in protein expression in NAc and DLPFC (Supplementary Fig. S2), with little overlap between rhythmic transcripts and proteins in NAc of both unaffected and OUD subjects.

In synaptosomes, robust protein expression rhythms were found in NAc (Fig. 4a) and DLPFC (Fig. 4e) of unaffected subjects. Rhythmic proteins in synaptosomes of unaffected subjects were significantly disrupted in subjects with OUD across both brain regions (Figs. 4a,e; Supplementary Tables S13-S24). Notably, there was very little overlap between rhythmic transcripts [2] and rhythmic proteins in either brain region of unaffected and OUD subjects (Fig. 4d, NAc; Fig 4h, DLPFC). The top rhythmic proteins

in NAc of unaffected subjects included the GABA transporter, GAT1 [91, 92] (Fig. 4b). In OUD subjects, two of the top rhythmic proteins included neurofilament proteins (NEFL, NEFM [93]; Fig. 4b), reflected by rhythmicity of actin and filament cytoskeleton organization pathways (Fig. 4c). When compared to unaffected subjects, the neuropeptide signaling pathway was also enriched among rhythmic proteins in NAc of OUD subjects (Fig. 4c), a pathway that involves upstream initiation by G protein-coupled receptor binding to opioid receptors and downstream activation of intracellular pathways. Indeed, significant rhythms in NAc synaptosomes of OUD subjects were found in several opioid peptides, including PDYN (prodynorphin) and PENK (proenkephalin) [94, 95], and other proteins involved in opioid receptor signaling (SCG5 [96] and PCSK1N [97]). SCG5 and PCSK1N are also secretory proteins also involved in preventing the aggregation of proteins involved in neurodegenerative disorders.

Moreover, CHID1 [98] and SPCS2 [99] were among the top rhythmic synaptic proteins in DLPFC of OUD subjects (Fig. 4f), both of which are linked to cytoskeletal pathology in neurodegenerative disorders. Enrichment analyses of rhythmic synaptic proteins in DLPFC in OUD subjects revealed pathways primarily associated with Golgi and endoplasmic reticulum processing, autophagy, glycosylation, and synaptic vesicle transport (Fig. 4g). Disrupted endoplasmic reticulum signaling, along with changes in the process of protein glycosylation, may reflect the impact of opioids on local protein translation and trafficking at postsynaptic sites, including dendritic spines, that ultimately regulate synaptic plasticity [100].

Altered Diurnal Rhythms of the Synaptic Proteome in DLPFC and NAc associated with OUD

At the synaptic level, rhythmic proteins were largely distinct between unaffected and OUD subjects. Given this, we examined whether proteins lost or gained rhythms between unaffected and OUD subjects within each brain region and sample preparation (Homogenates: Supplementary Figs. S1, S2 and Supplementary Tables S21, S22; Synaptosomes: NAc, Fig. 5a; DLPFC, Fig. 5d; Supplementary Tables S23, S24). In NAc homogenates, 5 proteins lost rhythms and 19 proteins gained rhythms, mostly involved in protein translation (Supplementary Fig. S2). Only 10 proteins displayed significantly altered expression rhythms in DLPFC homogenates between unaffected and OUD subjects, related to organophosphate biosynthesis processes involved in lipid homeostasis and neurotoxicity potentially involved in neurodegeneration (Supplementary Fig. S2).

In synaptosomes, 23 proteins lost rhythmicity in NAc of OUD subjects (*e.g.,* TRAPPC10, EHBP1, ZW10; Fig. 5a,b). Loss of protein rhythms in NAc were enriched for endoplasmic reticulum to Golgi vesicle-mediated transport pathways (Fig. 5c). In DLPFC, we found 7 synaptic proteins that lost rhythmicity in OUD and 11 synaptic proteins that gained rhythmicity (Fig. 5D; *e.g.,* USO1, NSDHL, PDE1C [101], Fig. 5E). Altered rhythmicity of synaptic proteins in DLPFC were associated with platelet-derived growth factor receptor beta (PDGFR-B) signaling, implicated in both neuroprotection in response to elevated glutamatergic activity [102] and opioid reward [103, 104]. Collectively, our findings suggest circadian rhythm regulation of the synaptic proteome that is significantly altered in a brain region-specific manner in OUD. Further, circadian disruption of synaptic

functions in OUD may primarily alter signaling pathways involved in endoplasmic reticulum-mediated local protein translation, trafficking, and vesicle endocytosis at the synapse, in addition to processes of neuroprotection and neurodegeneration.

Protein Co-Expression Modules Identify Brain Region-Specific Alterations in Circadian Rhythm Signaling and Synaptic Functions associated with OUD

Using weighted co-expression analyses, we identified highly connected protein expression modules specific to NAc and DLPFC in homogenates (Supplementary Figs. S3, S5, S7; Supplementary Table S25) and synaptosomes (Supplementary Figs. S4, S6, S8; Supplementary Table S25). To further narrow modules relevant for OUD associated protein alterations, we used MDC analysis, which examined the overall connectivity of protein co-expression and network structure between unaffected and OUD subjects.

Many modules in unaffected subjects displayed a loss of connectivity in NAc and DLPFC homogenates (Supplementary Fig. S9; Supplementary Table S26) and synaptosomes (Fig. 6). In synaptosomes, connectivity was significantly lost in 13/15 modules in the NAc of OUD subjects (Fig. 6a), along with 10/26 modules in DLPFC (Fig. 6b). We then investigated whether modules with changes in connectivity were enriched for hub proteins that were specific to unaffected and OUD groups and circadian rhythms. Focusing on the modules that lost connectivity in OUD, we found significant enrichment of both hub proteins specific to and/or rhythmic in unaffected subjects (Fig. 6). In NAc, there were three modules which lost connectivity in OUD that were significantly enriched for hub proteins (turquoise, green yellow, and green; Fig. 6a). In the green module, proteins are associated with various processes of synaptic plasticity, dendritic spine

formation, and axon guidance (*e.g.,* ROCK2 [105], DPYSL5 [106, 107], PLCG1 [108, 109], GDAP1 [110]; Fig. 6a). In the green yellow module, several of the rhythmic hub proteins were related to glutamatergic (GRIA2 [111–113]), GABAergic (GABRA2 [114–116]), and calcium signaling (CAMK2B, CALB2) (Fig. 6a). Additionally, other hub proteins are involved in calcium signaling, membrane potential, glutamatergic signaling, and exocytosis of synaptic vesicles (rhythmic hub SCAMP5; hubs SYNGR3 and LRRC7; Fig. 6a). Overall, protein networks that lost connectivity in the NAc of OUD subjects were mainly enriched for hub proteins that exhibited rhythmicity in unaffected subjects and involved in various synaptic processes, primarily GABAergic and glutamatergic neurotransmission (Fig. 6c).

In DLPFC, we identified two modules that lost connectivity in OUD, also with significant hub protein enrichments (Fig. 6b). The black module contained several highly connected hub proteins involved in ECM formation (LAMC1 [117]), presynaptic dopamine release (PLPP3 [118]), neuroprotection (NCEH1 [119], BCL2CL13), inflammation (LRRFIP2 [120]), and pronociceptive receptor signaling in pain (PIP5KL1 [121]). The green module contained several rhythmic hub proteins involved neuronal protection (NME3, SPHK2 [122], RAB13), synaptic functions (MCTP1, NTNG2, GNG5), and transposon activity in the brain (PGBD5 [123]) (Fig. 6b). Enrichment analysis primarily highlighted synaptic functions of vesicle cycling and structure (Fig. 6d). Collectively, our analyses lend further support for a role of circadian rhythms of synaptic signaling in human brain and the disruption of circadian-dependent regulation of various synaptic functions in OUD.

Discussion

Our previous transcriptomic findings implicate circadian rhythm disruption in proinflammatory signaling and synaptic remodeling in human NAc and DLPFC in OUD [2, 3]. We extend these findings here by showing significant alterations in circadian rhythm, GABAergic, and glutamatergic synaptic processes in both regions of OUD subjects. Using high-density profiling of peptides in tissue homogenates and synaptosomes within brain regions from the same subjects, we were able to identify and parse significant OUD-associated changes in synaptic proteomes specific to and common to NAc and DLPFC. In NAc synaptosomes specifically, pathways were involved in inflammatory, mitochondria, and metabolic signaling. In DLPFC synaptosomes from OUD subjects, pathways were mainly related to significant alterations in inflammatory signaling and serotonergic, dopaminergic, cholinergic, oxytocin neurotransmission. In both brain regions, pathways related to neurodegeneration, GABAergic and glutamatergic synapses, and circadian rhythms were associated with OUD, further supporting a role for circadian rhythms in synaptic signaling in opioid addiction.

Pathways related to neurodegeneration were common between differentially expressed proteins in NAc and DLPFC among tissue homogenates and synaptosomes in OUD. The relationship between chronic opioid use and increased risk for neurodegenerative disorders is seemingly complex. Several studies have reported increased risk of dementia and higher incidence of neurodegenerative disorders in people with heavy, chronic opioid use [124–126]. Chronic opioid use and dysfunction of the opioid system in the brain may contribute to neuroinflammation and the hyperphosphorylation of tau, a key protein involved in the pathogenesis of Alzheimer's

disease [126]. For example, dysfunction of opioid receptor signaling leads to increased amyloid beta expression and deposition [124]. Accumulation of amyloid beta is involved in the neurotoxicity observed early in the development of Alzheimer's disease.

Consistent with the emergence of early pathogenesis associated with neurodegenerative disorders, several studies have shown significant elevation of early markers of neuropathology in Alzheimer's disease in subjects who chronically used heroin, including hyperphosphorylated tau and amyloid beta [126]. Neurodegenerative markers in the brain were positively correlated with neuroinflammatory markers and microglial activation. Intriguingly, levels of the enzyme that phosphorylates tau, GSK-3B, were also increased in the same subjects [126]. We identified GSK-3B as a synaptically-enriched protein significantly upregulated in NAc and to a lesser degree in DLPFC of OUD subjects. Other related proteins were changed in both regions, including reduced expression of CBR1, BIN1, and VPS29 in DLPFC synaptosomes and reduced expression of SIRT2 in NAc synaptosomes. CBR1 is usually elevated in response to neuroinflammation and neuronal injury, ultimately facilitating neuroprotection [127]. Reduced BIN1 expression and function is a known risk factor for late-onset Alzheimer's disease, having critical roles in presynaptic release of glutamate and the facilitation of learning and memory [128]. Further, VPS29 is involved in synaptic survival [129]. OUD-associated downregulation of each of these proteins in DLPFC may reflect the initiation of molecular signaling cascades resembling early pathogenesis of Alzheimer's disease. In addition, SIRT2 downregulation in NAc synapses could lead to augmented activity at excitatory synapses via dysfunction of AMPA and NMDA glutamate receptors [130–132]. Accumulation of phosphorylated tau and other markers of neurodegenerative diseases,

accompanied by elevated neuroinflammation in the brain, likely have functional impacts on synaptic processes in NAc and DLPFC in OUD. In OUD, several synaptic proteins were enriched in both DLPFC and NAc that link neurotoxicity to augmented glutamatergic neurotransmission–CNTFR, PLXNA4, and SLC3A2. Although speculative, alterations in synaptic processes we highlighted here in subjects with OUD, particularly GABAergic and glutamatergic neurotransmission, may be associated with cognitive, mood, and reward dysfunction associated with opioid addiction.

An imbalance of GABAergic and glutamatergic signaling in NAc and DLPFC has been linked to OUD [112, 133]and other psychiatric disorders [134]. Between NAc and DLPFC of OUD subjects, our analyses identified several of the most impacted pathways in synaptosomes including GABAergic and glutamatergic neurotransmission. Several notable proteins involved in glutamatergic excitatory synapses were upregulated in DLPFC synaptosomes–GRIN2A (glutamate ionotropic receptor NMDA type subunit 2A), GRIN2B (glutamate ionotropic receptor NMDA type subunit 2A), GRM1 (glutamate metabotropic receptor 1), and SHANK2 (SH3 and multiple ankyrin repeat domains 2). GRIN proteins are subunits of the NMDA receptor complex, both of which are intimately involved in opioid-induced excitatory synaptic plasticity, having integral roles in opioid withdrawal and craving [135–137]. Synaptic elevation of SHANK2 may elevate NMDA receptor activity and enhance bursting of parvalbumin-positive neurons in DLPFC [138]. Enhancing NMDA receptor activation impairs synaptic plasticity and leads to cognitive impairments. We identified other synapse-specific proteins in the NAc involved in NMDA-dependent glutamate signaling, such as FLOT2 (upregulated), HDAC11 (downregulated), and SLC18B1 (downregulated). Notably, reduced HDAC11 expression in OUD and

function may impede synaptic plasticity [139]. CACNA2D1, SLC3A2, and GSK3B [68, 140], among others, were also enriched in both NAc and DLPFC of OUD subjects, each of which have dynamic roles in the regulation of glutamatergic-dependent synaptic plasticity [66, 67, 69]. In addition, proteins involved in GABAergic processes were also significantly altered in OUD. For example, GAD2 was reduced in DLPFC synaptosomes in subjects with OUD. GAD2 is associated with synaptic vesicle response during intense neuronal activity to release GABA into the synaptic cleft [141], consistent with dysfunctional inhibitory neurotransmission in opioid addiction.

Additionally, we identified proteins specifically altered in NAc and DLPFC of OUD subjects. For example, LSAMP and LY6H were more enriched in NAc synaptosomes, both of which are involved in dendritic spine formation in response to excitatory inputs. Other proteins related to neuroinflammation were upregulated in NAc (*e.g.,* HLA-B, GSTT1, S100A9). In DLPFC, synaptic enriched proteins included IGLON5, a neuronal adhesion molecule linked to neurological disorder characterized by sleep disorders and cognitive impairments; EPHA4 [142], a receptor tyrosine kinase that modulates aberrant synaptic functions in response to neuronal injury and neuroinflammation; and GPC1, a glycoprotein involved in extracellular matrix (ECM) formation. Several proteins with the highest fold-change in OUD subjects included keratin cytoskeletal, ECM-related proteins in NAc [143]. Reduced expression and function of keratin proteins and neurofilaments are associated with neuropsychiatric disorders [125,126], including stress-related disorders and substance use disorders [43]. The co-occurence of changes in proteins involved in the activation of neuroinflammatory processes, degradation of ECM, and synaptic remodeling corroborates our previous transcriptomic findings in opioid addiction [3].

Pathway analysis implicated circadian rhythm disruption primarily in synaptosomes of OUD subjects. However, protein expression rhythms were markedly disrupted in both homogenates and synaptosomes from NAc and DLPFC. For example, DARPP-32, a protein highly expressed in striatal medium spiny neurons [146–149], was highly rhythmic in NAc homogenates, suggesting opioid-induced circadian reprogramming of molecular cascades in the striatum [150]. Notably, opioid signaling was a top pathway that was rhythmic in NAc homogenates, where rhythms in opioidergic neurotransmission may contribute to craving and relapse [151, 152]. Proteins that lost rhythmicity in the NAc of OUD subjects were involved in membrane trafficking and endoplasmic reticulum to Golgi vesicle-mediated transport (*e.g.,* TRAPPC5, TRAPPC10, EHBP1, ZW10). Both TRAPPC5 and TRAPPC10 are transmembrane proteins of the cis-Golgi complex that support vesicular transport from endoplasmic reticulum to Golgi. TRAPP10 interacts with TRAPPC9 to form TRAPP II core proteins. TRAPPC9/10 proteins regulate the endocytic receptor recycling of dopamine 1 and 2 receptors in postsynaptic striatal medium spiny neurons [153], integral to regulation of medium spiny neuron physiology and motivated behaviors. Local translation at synaptic sites may also occur through activity-dependent transport [154]. Glycoproteins THY1 and NCAM1 [155] were highly rhythmic in DLPFC homogenates. An area of future work could explore the impact of opioids on protein glycosylation of synaptic proteins and their impact of synaptic vesicle loading and release [156], particularly glutamate receptor turnover and activation [113] in response to neuroinflammation [157, 158]. In addition, PDGFR-B signaling was among the top pathways from altered rhythms in protein expression of DLPFC synaptosomes in OUD. Importantly, PDGF-dependent signaling is involved in numerous opioid actions,

including tolerance [103, 104] and reward [159]. PDGF is a receptor tyrosine kinase, suggesting interactions between tyrosine kinases and opioid receptors may directly modulate glutamate receptor activity [160] depending on their circadian regulation.

Co-expression analyses revealed further insights into role of circadian rhythm regulation of synaptic dysfunction in OUD. We identified several protein modules that were enriched for rhythmic proteins and hub proteins involved in synaptic processes in unaffected subjects (*e.g.,* CAMK2B, GSK-3B, ROCK2, PLCG1, SCAMP5, SYT17). Each of which are involved in dendritic spine formation and synaptic plasticity [105, 161]. Every highly connected module in unaffected subjects in NAc and DLPFC lost connectivity in OUD subjects. Loss of connectivity in these protein networks in OUD could resemble a lack of coordinated protein signaling at the synapse that is modulated by circadian rhythms. OUD-associated upregulation of GSK-3B in synaptosomes of NAc and DLPFC likely leads to significant molecular rhythm disruptions in synapses, with potential consequences on activity-dependent synaptic plasticity [68, 140], and thus, may be a lynchpin in opioid and circadian actions at the synapse.

Overall, our findings implicate circadian rhythm disruption in altered functions at GABAergic and glutamatergic synapses in both NAc and DLPFC. Considering the role of sleep and circadian rhythms in opioid reward, craving, and relapse, treatments that target circadian pathways may be an effective therapeutic strategy for OUD.

Acknowledgments

Thank you to the staff and technicians who work diligently as part of the Brain Tissue Donation Program at the University of Pittsburgh. Postmortem human brain tissue was provided by the University of Pittsburgh Brain Tissue Donation Program and the National Institutes of Health NeuroBioBank at the University of Pittsburgh.

Author Contributions

MLS and RWL obtained funding for the project. JRG, DAL, MLS, MLM, and RWL designed and coordinated the study. SP, RS, MAS, MAH, SMK, JRG, and MLM processed samples for proteomics. SP, XX, ZF, GCT, AY, MLM, and RWL conducted analyses and data interpretation. SP, XX, MLS MLM, and RWL wrote the manuscript. All authors read and approved the final version of the manuscript.

Funding

The research reported in this article was supported by: Hamilton Family Prize for Basic Neuroscience Research in Psychiatry at the University of Pittsburgh School of Medicine (RWL); National Heart, Lung, and Blood Institute (R01HL150432, RWL); and National Institute on Drug Abuse (R01DA051390, MLS and RWL).

Competing Interests

The authors report no competing interests.

References

1. Abuse NI on D. Drug Overdose Death Rates. National Institute on Drug Abuse. 2023. https://nida.nih.gov/research-topics/trends-statistics/overdose-death-rates. Accessed 23 March 2023.

2. Xue X, Zong W, Glausier JR, Kim S-M, Shelton MA, Phan BN, et al. Molecular rhythm alterations in prefrontal cortex and nucleus accumbens associated with opioid use disorder. Transl Psychiatry. 2022;12:1–13.

3. Seney ML, Kim S-M, Glausier JR, Hildebrand MA, Xue X, Zong W, et al. Transcriptional Alterations in Dorsolateral Prefrontal Cortex and Nucleus Accumbens Implicate Neuroinflammation and Synaptic Remodeling in Opioid Use Disorder. Biological Psychiatry. 2021;90:550–562.

4. Nagamatsu ST, Rompala G, Hurd YL, Núñez-Rios DL, Montalvo-Ortiz JL, Traumatic Stress Brain Research Group. CpH methylome analysis in human cortical neurons identifies novel gene pathways and drug targets for opioid use disorder. Front Psychiatry. 2022;13:1078894.

5. Jacobs MM, Ökvist A, Horvath M, Keller E, Bannon MJ, Morgello S, et al. Dopamine receptor D1 and postsynaptic density gene variants associate with opiate abuse and striatal expression levels. Mol Psychiatry. 2013;18:1205–1210.

6. Sillivan SE, Whittard JD, Jacobs MM, Ren Y, Mazloom AR, Caputi FF, et al. ELK1 transcription factor linked to dysregulated striatal mu opioid receptor signaling network and OPRM1 polymorphism in human heroin abusers. Biol Psychiatry. 2013;74:511–519.

7. Brown TG, Xu J, Hurd YL, Pan Y-X. Dysregulated expression of the alternatively spliced variant mRNAs of the mu opioid receptor gene, OPRM1, in the medial prefrontal cortex of male human heroin abusers and heroin self-administering male rats. J Neurosci Res. 2022;100:35–47.

8. Valeri J, O'Donovan SM, Wang W, Sinclair D, Bollavarapu R, Gisabella B, et al. Altered expression of somatostatin signaling molecules and clock genes in the hippocampus of subjects with substance use disorder. Front Neurosci. 2022;16:903941.

9. Baldo BA. Prefrontal Cortical Opioids and Dysregulated Motivation: A Network Hypothesis. Trends Neurosci. 2016;39:366–377.

10. Adinoff B, Rilling LM, Williams MJ, Schreffler E, Schepis TS, Rosvall T, et al. Impulsivity, neural deficits, and the addictions: the 'oops' factor in relapse. J Addict Dis. 2007;26 Suppl 1:25–39.

11. Koob GF. Neurobiology of Opioid Addiction: Opponent Process, Hyperkatifeia, and Negative Reinforcement. Biol Psychiatry. 2020;87:44–53.

12. Grimm SL, Mendez EF, Stertz L, Meyer TD, Fries GR, Gandhi T, et al. MicroRNA-mRNA networks are dysregulated in opioid use disorder postmortem brain: Further evidence for opioid-induced neurovascular alterations. Front Psychiatry. 2022;13:1025346.

13. Mendez EF, Wei H, Hu R, Stertz L, Fries GR, Wu X, et al. Angiogenic gene networks are dysregulated in opioid use disorder: evidence from multi-omics and imaging of postmortem human brain. Mol Psychiatry. 2021;26:7803–7812.

14. Mahfoud Y, Talih F, Streem D, Budur K. Sleep disorders in substance abusers: how common are they? Psychiatry (Edgmont). 2009;6:38–42.

15. Huhn AS, Finan PH, Gamaldo CE, Hammond AS, Umbricht A, Bergeria CL, et al. Suvorexant ameliorated sleep disturbance, opioid withdrawal, and craving during a buprenorphine taper. Sci Transl Med. 2022;14:eabn8238.

16. Huhn AS, Ellis JD, Dunn KE, Sholler DJ, Tabaschek P, Burns R, et al. Patient-reported sleep outcomes in randomized-controlled trials in persons with substance use disorders: A systematic review. Drug Alcohol Depend. 2022;237:109508.

17. Eacret D, Veasey SC, Blendy JA. Bidirectional Relationship between Opioids and Disrupted Sleep: Putative Mechanisms. Mol Pharmacol. 2020;98:445–453.

18. Eacret D, Manduchi E, Noreck J, Tyner E, Fenik P, Dunn AD, et al. Mu-opioid receptor-expressing neurons in the paraventricular thalamus modulate chronic morphine-induced wake alterations. Transl Psychiatry. 2023;13:78.

19. Oyefeso A, Sedgwick P, Ghodse H. Subjective sleep-wake parameters in treatment-seeking opiate addicts. Drug Alcohol Depend. 1997;48:9–16.

20. Stinus L, Robert C, Karasinski P, Limoge A. Continuous quantitative monitoring of spontaneous opiate withdrawal: locomotor activity and sleep disorders. Pharmacol Biochem Behav. 1998;59:83–89.

21. Li S, Shi J, Epstein DH, Wang X, Zhang X, Bao Y, et al. Circadian alteration in neurobiology during 30 days of abstinence in heroin users. Biol Psychiatry. 2009;65:905–912.

22. Cao M, Javaheri S. Effects of Chronic Opioid Use on Sleep and Wake. Sleep Med Clin. 2018;13:271–281.

23. MacDonald ML, Garver M, Newman J, Sun Z, Kannarkat J, Salisbury R, et al. Synaptic Proteome Alterations in the Primary Auditory Cortex of Individuals With Schizophrenia. JAMA Psychiatry. 2020;77:86–95.

24. Dumrongprechachan V, Salisbury RB, Butler L, MacDonald ML, Kozorovitskiy Y. Dynamic proteomic and phosphoproteomic atlas of corticostriatal axons in neurodevelopment. Elife. 2022;11:e78847.

25. Dumrongprechachan V, Salisbury RB, Soto G, Kumar M, MacDonald ML, Kozorovitskiy Y. Cell-type and subcellular compartment-specific APEX2 proximity labeling reveals activity-dependent nuclear proteome dynamics in the striatum. Nat Commun. 2021;12:4855.

26. Glausier JR, Kelly MA, Salem S, Chen K, Lewis DA. Proxy measures of premortem cognitive aptitude in postmortem subjects with schizophrenia. Psychol Med. 2020;50:507–514.

27. Volk DW, Matsubara T, Li S, Sengupta EJ, Georgiev D, Minabe Y, et al. Deficits in Transcriptional Regulators of Cortical Parvalbumin Neurons in Schizophrenia. Am J Psychiatry. 2012;169:1082–1091.

28. Hashimoto T, Bazmi HH, Mirnics K, Wu Q, Sampson AR, Lewis DA. Conserved regional patterns of GABA-related transcript expression in the neocortex of subjects with schizophrenia. Am J Psychiatry. 2008;165:479–489.

29. Hahn C-G, Banerjee A, Macdonald ML, Cho D-S, Kamins J, Nie Z, et al. The post-synaptic density of human postmortem brain tissues: an experimental study paradigm for neuropsychiatric illnesses. PLoS One. 2009;4:e5251.

30. MacDonald ML, Ciccimaro E, Prakash A, Banerjee A, Seeholzer SH, Blair IA, et al. Biochemical Fractionation and Stable Isotope Dilution Liquid Chromatography-mass Spectrometry for Targeted and Microdomain-specific Protein Quantification in Human Postmortem Brain Tissue. Mol Cell Proteomics. 2012;11:1670–1681.

31. Zecha J, Satpathy S, Kanashova T, Avanessian SC, Kane MH, Clauser KR, et al. TMT Labeling for the Masses: A Robust and Cost-efficient, In-solution Labeling Approach. Mol Cell Proteomics. 2019;18:1468–1478.

32. Perez-Riverol Y, Bai J, Bandla C, García-Seisdedos D, Hewapathirana S, Kamatchinathan S, et al. The PRIDE database resources in 2022: a hub for mass spectrometry-based proteomics evidences. Nucleic Acids Res. 2021;50:D543–D552.

33. Browne CJ, Futamura R, Minier-Toribio A, Hicks EM, Ramakrishnan A, Martínez-Rivera F, et al. Transcriptional signatures of heroin intake and seeking throughout the brain reward circuit. BioRxiv. 2023:2023.01.11.523688.

34. Mews P, Cunningham AM, Scarpa J, Ramakrishnan A, Hicks EM, Bolnick S, et al. Convergent abnormalities in striatal gene networks in human cocaine use disorder and mouse cocaine administration models. Sci Adv. 2023;9:eadd8946.

35. Yu G, Wang L-G, Han Y, He Q-Y. clusterProfiler: an R package for comparing biological themes among gene clusters. OMICS. 2012;16:284–287.

36. Yu G, He Q-Y. ReactomePA: an R/Bioconductor package for reactome pathway analysis and visualization. Mol Biosyst. 2016;12:477–479.

37. Zhou Y, Zhou B, Pache L, Chang M, Khodabakhshi AH, Tanaseichuk O, et al.

Metascape provides a biologist-oriented resource for the analysis of systems-level datasets. Nat Commun. 2019;10:1523.

38. Langfelder P, Horvath S. WGCNA: an R package for weighted correlation network analysis. BMC Bioinformatics. 2008;9:559.

39. Langfelder P, Zhang B, Horvath S. Defining clusters from a hierarchical cluster tree: the Dynamic Tree Cut package for R. Bioinformatics. 2008;24:719–720.

40. Zhang B, Horvath S. A general framework for weighted gene co-expression network analysis. Stat Appl Genet Mol Biol. 2005;4:Article17.

41. Margolin AA, Nemenman I, Basso K, Wiggins C, Stolovitzky G, Dalla Favera R, et al. ARACNE: an algorithm for the reconstruction of gene regulatory networks in a mammalian cellular context. BMC Bioinformatics. 2006;7 Suppl 1:S7.

42. Koopmans F, van Nierop P, Andres-Alonso M, Byrnes A, Cijsouw T, Coba MP, et al. SynGO: An Evidence-Based, Expert-Curated Knowledge Base for the Synapse. Neuron. 2019;103:217-234.e4.

43. Morrison KE, Stenson AF, Marx-Rattner R, Carter S, Michopoulos V, Gillespie CF, et al. Developmental Timing of Trauma in Women Predicts Unique Extracellular Vesicle Proteome Signatures. Biol Psychiatry. 2022;91:273–282.

44. Javitt A, Barnea E, Kramer MP, Wolf-Levy H, Levin Y, Admon A, et al. Pro-inflammatory Cytokines Alter the Immunopeptidome Landscape by Modulation of HLA-B Expression. Frontiers in Immunology. 2019;10.

45. Liang TW, Chiu HH, Gurney A, Sidle A, Tumas DB, Schow P, et al. Vascular endothelial-junctional adhesion molecule (VE-JAM)/JAM 2 interacts with T, NK, and dendritic cells through JAM 3. J Immunol. 2002;168:1618–1626.

46. Koss H, Bunney TD, Behjati S, Katan M. Dysfunction of phospholipase Cγ in immune disorders and cancer. Trends Biochem Sci. 2014;39:603–611.

47. Sabbir MG, Speth RC, Albensi BC. Loss of Cholinergic Receptor Muscarinic 1 (CHRM1) Protein in the Hippocampus and Temporal Cortex of a Subset of Individuals with Alzheimer's Disease, Parkinson's Disease, or Frontotemporal Dementia: Implications for Patient Survival. J Alzheimers Dis. 2022;90:727–747.

48. Zhu G, Fang Y, Cui X, Jia R, Kang X, Zhao R. Magnolol upregulates CHRM1 to attenuate Amyloid-β-triggered neuronal injury through regulating the cAMP/PKA/CREB pathway. J Nat Med. 2022;76:188–199.

49. Strang KH, Golde TE, Giasson BI. MAPT mutations, tauopathy, and mechanisms of neurodegeneration. Lab Invest. 2019;99:912–928.

50. Ma S, Attarwala IY, Xie X-Q. SQSTM1/p62: A Potential Target for Neurodegenerative Disease. ACS Chem Neurosci. 2019;10:2094–2114.

51. Aykac A, Sehirli AO. The Role of the SLC Transporters Protein in the Neurodegenerative Disorders. Clin Psychopharmacol Neurosci. 2020;18:174–187.

52. Chee LY, Cumming A. Polymorphisms in the Cholinergic Receptors Muscarinic (CHRM2 and CHRM3) Genes and Alzheimer's Disease. Avicenna J Med Biotechnol. 2018;10:196–199.

53. Querfurth H, Lee H-K. Mammalian/mechanistic target of rapamycin (mTOR) complexes in neurodegeneration. Molecular Neurodegeneration. 2021;16:44.

54. Foskett JK. Inositol trisphosphate receptor Ca2+ release channels in neurological diseases. Pflugers Arch. 2010;460:481–494.

55. Lokireddy S, Kukushkin NV, Goldberg AL. cAMP-induced phosphorylation of 26S proteasomes on Rpn6/PSMD11 enhances their activity and the degradation of misfolded proteins. Proc Natl Acad Sci U S A. 2015;112:E7176–E7185.

56. Huang Z-N, Her L-S. The Ubiquitin Receptor ADRM1 Modulates HAP40-Induced Proteasome Activity. Mol Neurobiol. 2017;54:7382–7400.

57. Benkler C, O'Neil AL, Slepian S, Qian F, Weinreb PH, Rubin LL. Aggregated SOD1 causes selective death of cultured human motor neurons. Sci Rep. 2018;8:16393.

58. Heremans IP, Caligiore F, Gerin I, Bury M, Lutz M, Graff J, et al. Parkinson's disease protein PARK7 prevents metabolite and protein damage caused by a glycolytic metabolite. Proceedings of the National Academy of Sciences. 2022;119:e2111338119.

59. Plun-Favreau H, Klupsch K, Moisoi N, Gandhi S, Kjaer S, Frith D, et al. The mitochondrial protease HtrA2 is regulated by Parkinson's disease-associated kinase PINK1. Nat Cell Biol. 2007;9:1243–1252.

60. Shi Q, Li J-L, Ma Y, Gao L-P, Xiao K, Wang J, et al. Decrease of RyR2 in the prion infected cell line and in the brains of the scrapie infected mice models and the patients of human prion diseases. Prion. 2018;12:175–184.

61. Bradley JA, Ramirez G, Hagood JS. Roles and Regulation of Thy-1, a Context-Dependent Modulator of Cell Phenotype. Biofactors. 2009;35:258–265.

62. Jeng C-J, McCarroll SA, Martin TFJ, Floor E, Adams J, Krantz D, et al. Thy-1 Is a Component Common to Multiple Populations of Synaptic Vesicles. J Cell Biol. 1998;140:685–698.

63. Dahimene S, von Elsner L, Holling T, Mattas LS, Pickard J, Lessel D, et al. Biallelic CACNA2D1 loss-of-function variants cause early-onset developmental epileptic encephalopathy. Brain. 2022;145:2721–2729.

64. Grosso BJ, Kramer AA, Tyagi S, Bennett DF, Tifft CJ, D'Souza P, et al. Complex

effects on CaV2.1 channel gating caused by a CACNA1A variant associated with a severe neurodevelopmental disorder. Sci Rep. 2022;12:9186.

65. Luo X, Rosenfeld JA, Yamamoto S, Harel T, Zuo Z, Hall M, et al. Clinically severe CACNA1A alleles affect synaptic function and neurodegeneration differentially. PLoS Genet. 2017;13:e1006905.

66. Chen J, Li L, Chen S-R, Chen H, Xie J-D, Sirrieh RE, et al. The α2δ-1-NMDA Receptor Complex Is Critically Involved in Neuropathic Pain Development and Gabapentin Therapeutic Actions. Cell Reports. 2018;22:2307–2321.

67. Lin C-H, Lin P-P, Lin C-Y, Lin C-H, Huang C-H, Huang Y-J, et al. Decreased mRNA expression for the two subunits of system xc−, SLC3A2 and SLC7A11, in WBC in patients with schizophrenia: Evidence in support of the hypo-glutamatergic hypothesis of schizophrenia. Journal of Psychiatric Research. 2016;72:58–63.

68. Peineau S, Bradley C, Taghibiglou C, Doherty A, Bortolotto ZA, Wang YT, et al. The role of GSK-3 in synaptic plasticity. Br J Pharmacol. 2008;153:S428–S437.

69. Jaworski T. Control of neuronal excitability by GSK-3beta: Epilepsy and beyond. Biochimica et Biophysica Acta (BBA) - Molecular Cell Research. 2020;1867:118745.

70. Tyagarajan SK, Ghosh H, Yévenes GE, Nikonenko I, Ebeling C, Schwerdel C, et al. Regulation of GABAergic synapse formation and plasticity by GSK3beta-dependent phosphorylation of gephyrin. Proc Natl Acad Sci U S A. 2011;108:379–384.

71. Bregin A, Kaare M, Jagomäe T, Karis K, Singh K, Laugus K, et al. Expression and impact of Lsamp neural adhesion molecule in the serotonergic neurotransmission system. Pharmacol Biochem Behav. 2020;198:173017.

72. Bregin A, Mazitov T, Aug I, Philips M-A, Innos J, Vasar E. Increased sensitivity to psychostimulants and GABAergic drugs in Lsamp-deficient mice. Pharmacol Biochem Behav. 2019;183:87–97.

73. Moriwaki Y, Kubo N, Watanabe M, Asano S, Shinoda T, Sugino T, et al. Endogenous neurotoxin-like protein Ly6H inhibits alpha7 nicotinic acetylcholine receptor currents at the plasma membrane. Sci Rep. 2020;10:11996.

74. Puddifoot CA, Wu M, Sung R-J, Joiner WJ. Ly6h Regulates Trafficking of Alpha7 Nicotinic Acetylcholine Receptors and Nicotine-Induced Potentiation of Glutamatergic Signaling. J Neurosci. 2015;35:3420–3430.

75. Brennaman LH, Zhang X, Guan H, Triplett JW, Brown A, Demyanenko GP, et al. Polysialylated NCAM and EphrinA/EphA Regulate Synaptic Development of GABAergic Interneurons in Prefrontal Cortex. Cereb Cortex. 2013;23:162–177.

76. Chen HC, Loh HH. mu-Opioid receptor gene expression: the role of NCAM.

Neuroscience. 2001;108:7–15.

77. Duncan BW, Murphy KE, Maness PF. Molecular Mechanisms of L1 and NCAM Adhesion Molecules in Synaptic Pruning, Plasticity, and Stabilization. Front Cell Dev Biol. 2021;9:625340.

78. Nelson EC, Lynskey MT, Heath AC, Wray N, Agrawal A, Shand FL, et al. ANKK1, TTC12, and NCAM1 Polymorphisms and Heroin Dependence – importance of considering drug exposure. JAMA Psychiatry. 2013;70:325–333.

79. Polo-Parada L, Bose CM, Plattner F, Landmesser LT. Distinct Roles of Different Neural Cell Adhesion Molecule (NCAM) Isoforms in Synaptic Maturation Revealed by Analysis of NCAM 180 kDa Isoform-Deficient Mice. J Neurosci. 2004;24:1852–1864.

80. Bae Y-S, Chung W, Han K, Park KY, Kim H, Kim E, et al. Down-regulation of RalBP1 expression reduces seizure threshold and synaptic inhibition in mice. Biochem Biophys Res Commun. 2013;433:175–180.

81. Chen M-S, Kim H, Jagot-Lacoussiere L, Maurel P. Cadm3 (Necl-1) interferes with the activation of the PI3 kinase/Akt signaling cascade and inhibits Schwann cell myelination in vitro. Glia. 2016;64:2247–2262.

82. Seney ML, Chang L-C, Oh H, Wang X, Tseng GC, Lewis DA, et al. The Role of Genetic Sex in Affect Regulation and Expression of GABA-Related Genes Across Species. Front Psychiatry. 2013;4:104.

83. Kamimura K, Maeda N. Glypicans and Heparan Sulfate in Synaptic Development, Neural Plasticity, and Neurological Disorders. Front Neural Circuits. 2021;15:595596.

84. Beurrier C, Faideau M, Bennouar K-E, Escartin C, Kerkerian-Le Goff L, Bonvento G, et al. Ciliary Neurotrophic Factor Protects Striatal Neurons against Excitotoxicity by Enhancing Glial Glutamate Uptake. PLoS One. 2010;5:e8550.

85. Karis K, Eskla K-L, Kaare M, Täht K, Tuusov J, Visnapuu T, et al. Altered Expression Profile of IgLON Family of Neural Cell Adhesion Molecules in the Dorsolateral Prefrontal Cortex of Schizophrenic Patients. Front Mol Neurosci. 2018;11:8.

86. Wang Q, Chiu S-L, Koropouli E, Hong I, Mitchell S, Easwaran TP, et al. Neuropilin-2/PlexinA3 Receptors Associate with GluA1 and Mediate Sema3F-dependent Homeostatic Scaling in Cortical Neurons. Neuron. 2017;96:1084-1098.e7.

87. Yamashita N, Usui H, Nakamura F, Chen S, Sasaki Y, Hida T, et al. Plexin-A4-dependent retrograde semaphorin 3A signalling regulates the dendritic localization of GluA2-containing AMPA receptors. Nat Commun. 2014;5:3424.

88. Awasthi A, Ramachandran B, Ahmed S, Benito E, Shinoda Y, Nitzan N, et al.

Synaptotagmin-3 drives AMPA receptor endocytosis, depression of synapse strength, and forgetting. Science. 2019;363:eaav1483.

89. Lewis JE, Brameld JM, Jethwa PH. Neuroendocrine Role for VGF. Frontiers in Endocrinology. 2015;6.

90. Perez SM, Donegan JJ, Boley AM, Aguilar DD, Giuffrida A, Lodge DJ. Ventral hippocampal overexpression of Cannabinoid Receptor Interacting Protein 1 (CNRIP1) produces a schizophrenia-like phenotype in the rat. Schizophr Res. 2019;206:263–270.

91. Jin X-T, Galvan A, Wichmann T, Smith Y. Localization and Function of GABA Transporters GAT-1 and GAT-3 in the Basal Ganglia. Front Syst Neurosci. 2011;5:63.

92. Savtchenko L, Megalogeni M, Rusakov DA, Walker MC, Pavlov I. Synaptic GABA release prevents GABA transporter type-1 reversal during excessive network activity. Nat Commun. 2015;6:6597.

93. Yuan A, Rao MV, Veeranna, Nixon RA. Neurofilaments at a glance. J Cell Sci. 2012;125:3257–3263.

94. Nikoshkov A, Drakenberg K, Wang X, Horvath MCs, Keller E, Hurd YL. Opioid neuropeptide genotypes in relation to heroin abuse: Dopamine tone contributes to reversed mesolimbic proenkephalin expression. Proceedings of the National Academy of Sciences. 2008;105:786–791.

95. Kieffer BL, Gavériaux-Ruff C. Exploring the opioid system by gene knockout. Progress in Neurobiology. 2002;66:285–306.

96. Chaplot K, Jarvela TS, Lindberg I. Secreted Chaperones in Neurodegeneration. Front Aging Neurosci. 2020;12:268.

97. Ram A, Edwards T, McCarty A, Afrose L, McDermott MV, Bobeck EN. GPR171 Agonist Reduces Chronic Neuropathic and Inflammatory Pain in Male, But Not Female Mice. Frontiers in Pain Research. 2021;2.

98. Castrogiovanni P, Sanfilippo C, Imbesi R, Maugeri G, Lo Furno D, Tibullo D, et al. Brain CHID1 Expression Correlates with NRGN and CALB1 in Healthy Subjects and AD Patients. Cells. 2021;10:882.

99. Manavalan A, Mishra M, Feng L, Sze SK, Akatsu H, Heese K. Brain site-specific proteome changes in aging-related dementia. Exp Mol Med. 2013;45:e39–e39.

100. Chanaday NL, Kavalali ET. Role of the endoplasmic reticulum in synaptic transmission. Curr Opin Neurobiol. 2022;73:102538.

101. Rombaut B, Kessels S, Schepers M, Tiane A, Paes D, Solomina Y, et al. PDE inhibition in distinct cell types to reclaim the balance of synaptic plasticity. Theranostics. 2021;11:2080–2097.

102. Sil S, Periyasamy P, Thangaraj A, Chivero ET, Buch S. PDGF/PDGFR axis in the neural systems. Mol Aspects Med. 2018;62:63–74.

103. Puig S, Barker KE, Szott SR, Kann PT, Morris JS, Gutstein HB. Spinal Opioid Tolerance Depends upon Platelet-Derived Growth Factor Receptor-β Signaling, Not μ-Opioid Receptor Internalization. Mol Pharmacol. 2020;98:487–496.

104. Wang Y, Barker K, Shi S, Diaz M, Mo B, Gutstein HB. Blockade of PDGFR-β activation eliminates morphine analgesic tolerance. Nat Med. 2012;18:385–387.

105. Zhou Z, Meng Y, Asrar S, Todorovski Z, Jia Z. A critical role of Rho-kinase ROCK2 in the regulation of spine and synaptic function. Neuropharmacology. 2009;56:81–89.

106. Strawbridge RJ, Ward J, Lyall LM, Tunbridge EM, Cullen B, Graham N, et al. Genetics of self-reported risk-taking behaviour, trans-ethnic consistency and relevance to brain gene expression. Transl Psychiatry. 2018;8:1–11.

107. Jeanne M, Demory H, Moutal A, Vuillaume M-L, Blesson S, Thépault R-A, et al. Missense variants in DPYSL5 cause a neurodevelopmental disorder with corpus callosum agenesis and cerebellar abnormalities. The American Journal of Human Genetics. 2021;108:951–961.

108. Gawden-Bone CM, Frazer GL, Richard AC, Ma CY, Strege K, Griffiths GM. PIP5 Kinases Regulate Membrane Phosphoinositide and Actin Composition for Targeted Granule Secretion by Cytotoxic Lymphocytes. Immunity. 2018;49:427-437.e4.

109. Schaffer TB, Smith JE, Cook EK, Phan T, Margolis SS. PKCε Inhibits Neuronal Dendritic Spine Development through Dual Phosphorylation of Ephexin5. Cell Rep. 2018;25:2470-2483.e8.

110. Miressi F, Benslimane N, Favreau F, Rassat M, Richard L, Bourthoumieu S, et al. GDAP1 Involvement in Mitochondrial Function and Oxidative Stress, Investigated in a Charcot-Marie-Tooth Model of hiPSCs-Derived Motor Neurons. Biomedicines. 2021;9:945.

111. Russell SE, Puttick DJ, Sawyer AM, Potter DN, Mague S, Carlezon WA, et al. Nucleus Accumbens AMPA Receptors Are Necessary for Morphine-Withdrawal-Induced Negative-Affective States in Rats. J Neurosci. 2016;36:5748–5762.

112. Hearing M, Graziane N, Dong Y, Thomas MJ. Opioid and psychostimulant plasticity: targeting overlap in nucleus accumbens glutamate signaling. Trends Pharmacol Sci. 2018;39:276–294.

113. Ancona Esselmann SG, Díaz-Alonso J, Levy JM, Bemben MA, Nicoll RA. Synaptic homeostasis requires the membrane-proximal carboxy tail of GluA2. Proceedings of the National Academy of Sciences. 2017;114:13266–13271.

114. Mallard TT, Ashenhurst JR, Harden KP, Fromme K. GABRA2, alcohol, and illicit

drug use: an event-level model of genetic risk for polysubstance use. J Abnorm Psychol. 2018;127:190–201.

115. Enoch M-A, Hodgkinson CA, Yuan Q, Shen P-H, Goldman D, Roy A. The Influence of GABRA2, Childhood Trauma, and Their Interaction on Alcohol, Heroin, and Cocaine Dependence. Biological Psychiatry. 2010;67:20–27.

116. Sun Y, Zhang Y, Zhang D, Chang S, Jing R, Yue W, et al. GABRA2 rs279858-linked variants are associated with disrupted structural connectome of reward circuits in heroin abusers. Transl Psychiatry. 2018;8:1–10.

117. Nirwane A, Yao Y. Laminins and their receptors in the CNS. Biol Rev Camb Philos Soc. 2019;94:283–306.

118. Gómez-López S, Martínez-Silva AV, Montiel T, Osorio-Gómez D, Bermúdez-Rattoni F, Massieu L, et al. Neural ablation of the PARK10 candidate Plpp3 leads to dopaminergic transmission deficits without neurodegeneration. Sci Rep. 2016;6:24028.

119. Zhang S, Glukhova SA, Caldwell KA, Caldwell GA. NCEH-1 modulates cholesterol metabolism and protects against α-synuclein toxicity in a C. elegans model of Parkinson's disease. Hum Mol Genet. 2017;26:3823–3836.

120. Jin J, Yu Q, Han C, Hu X, Xu S, Wang Q, et al. LRRFIP2 negatively regulates NLRP3 inflammasome activation in macrophages by promoting Flightless-I-mediated caspase-1 inhibition. Nat Commun. 2013;4:2075.

121. Wright BD, Loo L, Street SE, Ma A, Taylor-Blake B, Stashko MA, et al. The lipid kinase PIP5K1C regulates pain signaling and sensitization. Neuron. 2014;82:836–847.

122. Dominguez G, Maddelein M-L, Pucelle M, Nicaise Y, Maurage C-A, Duyckaerts C, et al. Neuronal sphingosine kinase 2 subcellular localization is altered in Alzheimer's disease brain. Acta Neuropathologica Communications. 2018;6:25.

123. Pavelitz T, Gray LT, Padilla SL, Bailey AD, Weiner AM. PGBD5: a neural-specific intron-containing piggyBac transposase domesticated over 500 million years ago and conserved from cephalochordates to humans. Mobile DNA. 2013;4:23.

124. Cai Z, Ratka A. Opioid system and Alzheimer's disease. Neuromolecular Med. 2012;14:91–111.

125. Kennedy GJ. Bad News and Good: Opioids are Associated with the Incidence of Dementia, but the Effect is Substantial Only for Those 75-80 Years of Age. Am J Geriatr Psychiatry. 2023;31:324–325.

126. Anthony IC, Norrby KE, Dingwall T, Carnie FW, Millar T, Arango JC, et al. Predisposition to accelerated Alzheimer-related changes in the brains of human immunodeficiency virus negative opiate abusers. Brain. 2010;133:3685–3698.

127. Mao L, Wang K, Zhang P, Ren S, Sun J, Yang M, et al. Carbonyl Reductase 1 Attenuates Ischemic Brain Injury by Reducing Oxidative Stress and Neuroinflammation. Transl Stroke Res. 2021;12:711–724.

128. De Rossi P, Nomura T, Andrew RJ, Masse NY, Sampathkumar V, Musial TF, et al. Neuronal BIN1 Regulates Presynaptic Neurotransmitter Release and Memory Consolidation. Cell Rep. 2020;30:3520-3535.e7.

129. Ye H, Ojelade SA, Li-Kroeger D, Zuo Z, Wang L, Li Y, et al. Retromer subunit, VPS29, regulates synaptic transmission and is required for endolysosomal function in the aging brain. ELife;9:e51977.

130. Chen X, Lu W, Wu D. Sirtuin 2 (SIRT2): Confusing Roles in the Pathophysiology of Neurological Disorders. Front Neurosci. 2021;15:614107.

131. Ferguson D, Koo JW, Feng J, Heller E, Rabkin J, Heshmati M, et al. Essential Role of SIRT1 Signaling in the Nucleus Accumbens in Cocaine and Morphine Action. J Neurosci. 2013;33:16088–16098.

132. Wang G, Li S, Gilbert J, Gritton HJ, Wang Z, Li Z, et al. Crucial Roles for SIRT2 and AMPA Receptor Acetylation in Synaptic Plasticity and Memory. Cell Rep. 2017;20:1335–1347.

133. Hearing MC, Jedynak J, Ebner SR, Ingebretson A, Asp AJ, Fischer RA, et al. Reversal of morphine-induced cell-type-specific synaptic plasticity in the nucleus accumbens shell blocks reinstatement. Proc Natl Acad Sci U S A. 2016;113:757–762.

134. Sohal VS, Rubenstein JLR. Excitation-inhibition balance as a framework for investigating mechanisms in neuropsychiatric disorders. Mol Psychiatry. 2019;24:1248–1257.

135. Zhao B, Zhu Y, Wang W, Cui H, Wang Y, Lai J. Analysis of Variations in the Glutamate Receptor, N-Methyl D-Aspartate 2A (GRIN2A) Gene Reveals Their Relative Importance as Genetic Susceptibility Factors for Heroin Addiction. PLoS One. 2013;8:e70817.

136. Elmasri M, Lotti JS, Aziz W, Steele OG, Karachaliou E, Sakimura K, et al. Synaptic Dysfunction by Mutations in GRIN2B: Influence of Triheteromeric NMDA Receptors on Gain-of-Function and Loss-of-Function Mutant Classification. Brain Sci. 2022;12:789.

137. Sheng Z, Liu Q, Cheng C, Li M, Barash J, Kofke WA, et al. Fentanyl induces autism-like behaviours in mice by hypermethylation of the glutamate receptor gene Grin2b. British Journal of Anaesthesia. 2022;129:544–554.

138. Lee E, Lee S, Shin JJ, Choi W, Chung C, Lee S, et al. Excitatory synapses and gap junctions cooperate to improve Pv neuronal burst firing and cortical social cognition in Shank2-mutant mice. Nat Commun. 2021;12:5116.

139. Bryant DT, Landles C, Papadopoulou AS, Benjamin AC, Duckworth JK, Rosahl T, et al. Disruption to schizophrenia-associated gene Fez1 in the hippocampus of HDAC11 knockout mice. Sci Rep. 2017;7:11900.

140. Jaworski T, Banach-Kasper E, Gralec K. GSK-3β at the Intersection of Neuronal Plasticity and Neurodegeneration. Neural Plast. 2019;2019:4209475.

141. Glausier JR, Kimoto S, Fish KN, Lewis DA. Lower glutamic acid decarboxylase 65-kDa isoform messenger RNA and protein levels in the prefrontal cortex in schizoaffective disorder but not schizophrenia. Biol Psychiatry. 2015;77:167–176.

142. Kowalski EA, Chen J, Hazy A, Fritsch LE, Gudenschwager-Basso EK, Chen M, et al. Peripheral loss of EphA4 ameliorates TBI-induced neuroinflammation and tissue damage. Journal of Neuroinflammation. 2019;16:210.

143. Bott CJ, Winckler B. Intermediate filaments in developing neurons: Beyond structure. Cytoskeleton. 2020;77:110–128.

144. Yuan A, Nixon RA. Specialized roles of neurofilament proteins in synapses: Relevance to neuropsychiatric disorders. Brain Research Bulletin. 2016;126:334–346.

145. Radoja N, Komine M, Jho SH, Blumenberg M, Tomic-Canic M. Novel mechanism of steroid action in skin through glucocorticoid receptor monomers. Mol Cell Biol. 2000;20:4328–4339.

146. Borgkvist A, Usiello A, Greengard P, Fisone G. Activation of the cAMP/PKA/DARPP-32 Signaling Pathway is Required for Morphine Psychomotor Stimulation but not for Morphine Reward. Neuropsychopharmacol. 2007;32:1995–2003.

147. Gould TD, Manji HK. DARPP-32: A molecular switch at the nexus of reward pathway plasticity. Proceedings of the National Academy of Sciences. 2005;102:253–254.

148. Mahajan SD, Aalinkeel R, Reynolds JL, Nair BB, Sykes DE, Hu Z, et al. Therapeutic targeting of 'DARPP-32': a key signaling molecule in the dopiminergic pathway for the treatment of opiate addiction. Int Rev Neurobiol. 2009;88:199–222.

149. Svenningsson P, Nishi A, Fisone G, Girault J-A, Nairn AC, Greengard P. DARPP-32: an integrator of neurotransmission. Annu Rev Pharmacol Toxicol. 2004;44:269–296.

150. Brami-Cherrier K, Lewis RG, Cervantes M, Liu Y, Tognini P, Baldi P, et al. Cocaine-mediated circadian reprogramming in the striatum through dopamine D2R and PPARγ activation. Nat Commun. 2020;11:4448.

151. Bumgarner JR, McCray EW, Nelson RJ. The disruptive relationship among circadian rhythms, pain, and opioids. Frontiers in Neuroscience. 2023;17.

152. Gallerani M, Manfredini R, Dal Monte D, Calò G, Brunaldi V, Simonato M. Circadian differences in the individual sensitivity to opiate overdose. Crit Care Med. 2001;29:96–101.

153. Ke Y, Weng M, Chhetri G, Usman M, Li Y, Yu Q, et al. Trappc9 deficiency in mice impairs learning and memory by causing imbalance of dopamine D1 and D2 neurons. Sci Adv. 2020;6:eabb7781.

154. Carter SD, Hampton CM, Langlois R, Melero R, Farino ZJ, Calderon MJ, et al. Ribosome-associated vesicles: A dynamic subcompartment of the endoplasmic reticulum in secretory cells. Sci Adv. 2020;6:eaay9572.

155. Mauvoisin D, Wang J, Jouffe C, Martin E, Atger F, Waridel P, et al. Circadian clock-dependent and -independent rhythmic proteomes implement distinct diurnal functions in mouse liver. Proceedings of the National Academy of Sciences. 2014;111:167–172.

156. Conroy LR, Hawkinson TR, Young LEA, Gentry MS, Sun RC. Emerging roles of N-linked glycosylation in brain physiology and disorders. Trends Endocrinol Metab. 2021;32:980–993.

157. Weinhard L, di Bartolomei G, Bolasco G, Machado P, Schieber NL, Neniskyte U, et al. Microglia remodel synapses by presynaptic trogocytosis and spine head filopodia induction. Nat Commun. 2018;9:1228.

158. Calcia MA, Bonsall DR, Bloomfield PS, Selvaraj S, Barichello T, Howes OD. Stress and neuroinflammation: a systematic review of the effects of stress on microglia and the implications for mental illness. Psychopharmacology (Berl). 2016;233:1637–1650.

159. Gamble MC, Williams BR, Singh N, Posa L, Freyberg Z, Logan RW, et al. Mu-opioid receptor and receptor tyrosine kinase crosstalk: Implications in mechanisms of opioid tolerance, reduced analgesia to neuropathic pain, dependence, and reward. Front Syst Neurosci. 2022;16:1059089.

160. Nenadic I, Maitra R, Scherpiet S, Gaser C, Schultz CC, Schachtzabel C, et al. Glutamate receptor δ 1 (GRID1) genetic variation and brain structure in schizophrenia. J Psychiatr Res. 2012;46:1531–1539.

161. Lee U, Choi C, Ryu SH, Park D, Lee S-E, Kim K, et al. SCAMP5 plays a critical role in axonal trafficking and synaptic localization of NHE6 to adjust quantal size at glutamatergic synapses. Proceedings of the National Academy of Sciences. 2021;118:e2011371118.

Figure Legends

Figure 1. Proteomic alterations in tissue homogenates from NAc and DLPFC in subjects with OUD. a) Log_2FC plotted relative to $-log_{10}$ *p* value by volcano plot for DE proteins in NAc homogenates. **b**) Log_2FC plotted relative to $-log_{10}$ *p* value by volcano plot for DE proteins in DLPFC homogenates. Horizontal dashed lines represent *p* value significance cutoff of corrected $p < 0.05$, while vertical dashed lines represent log_2FC cutoffs of ≤ -0.26 or ≥ 0.26 (FC $\geq$ 1.2). Blue circles represent DE proteins that reach significance and log_2FC. **c**) RRHO plot indicating weak overlap or concordance of protein expression alterations in OUD between DLPFC and NAc. **d**) Venn diagrams of downregulated and upregulated proteins between NAc and DLPFC homogenates. **e**) Volcano plots for DE proteins in NAc synaptosomes. **f**) Volcano plots for DE proteins in DLPFC synaptosomes. **g**) RRHO plot indicating weak discordance of protein expression alterations in OUD between DLPFC and NAc synaptosomes. **h**) Venn diagrams of downregulated and upregulated proteins between NAc and DLPFC synaptosomes.

Figure 2. Differential enrichment of synaptic proteins between NAc and DLPFC associated with OUD. Lollipop plot showing pathways enriched from DE proteins in synaptosomes relative to homogenates in **a**) NAc and **b**) DLPFC. Adjusted p-value by color and size of circle represents counts of proteins within pathways. NAc, Nucleus Accumbens; DLPFC, Dorsolateral Prefrontal Cortex.

Figure 3. Alterations in protein synaptic enrichments in DLPFC and NAc associated with OUD. Heatmap highlighting top enriched proteins in NAc and DLPFC synaptosomes as compared to homogenates and differentially expressed in OUD. Warmer colors indicate increasing $-\log_{10} p$ value and highly enriched proteins in OUD synaptosomes. In contrast, cooler colors indicate decreasing $-\log_{10} p$ value and negative enrichment of proteins in OUD synaptosomes.

Figure 4. Diurnal rhythms of protein expression in DLPFC and NAc synaptosomes associated with OUD. a) Heatmaps highlighting top 200 rhythmic proteins from NAc synaptosomes of unaffected subjects. Rhythmic proteins in unaffected subjects are plotted in OUD subjects to show disruption of protein rhythmicity. Heatmaps were generated by performing supervised clustering of expression of top 200 rhythmic proteins found in homogenates from Unaffected subjects and applied to OUD. Subjects were ordered by TOD to visualize expression levels over a period of 24 hours. Yellow color indicates increased Z-score and higher protein expression, while blue color indicates decreased Z-score and lower protein expression. **b**) Scatterplots of top rhythmic proteins in NAc synaptosomes from unaffected and OUD subjects. Scatterplots were generated to represent expression rhythms for individual proteins. The x-axis represents TOD on the ZT scale and protein expression level is on y-axis, with each dot representing a subject. The red line is the fitted sinusoidal curve to reflect temporal rhythms. **c**) Pathway

enrichment analysis comparing rhythmic proteins in NAc synaptosomes from unaffected and OUD subjects. Warmer colors indicate increasing $-\log_{10} p$ value and highly rhythmic pathways in each group. **d**) Venn diagrams showing low overlap of rhythmic proteins and genes in NAc synaptosomes from unaffected and OUD subjects. **e**) Heatmaps highlighting top 200 rhythmic proteins from DLPFC synaptosomes of unaffected subjects. Rhythmic proteins in unaffected subjects are plotted in OUD subjects to show disruption of protein rhythmicity. **f**) Scatterplots of top rhythmic proteins in DLPFC synaptosomes from unaffected and OUD subjects. **g**) Pathway enrichment analysis comparing top 200 rhythmic proteins found in DLPFC synaptosomes from unaffected and OUD subjects. **h**) Venn diagrams showing low overlap of rhythmic proteins and genes in DLPFC synaptosomes from unaffected and OUD subjects. Also see Figure S1 for protein expression rhythm heatmaps in OUD. TOD, Time of Death; NAc, Nucleus Accumbens; DLPFC, Dorsolateral Prefrontal Cortex.

Figure 5. Altered rhythmicity of the synaptic proteome in DLPFC and NAc associated with OUD. Comparison of rhythmic proteins between unaffected and OUD subjects in synaptosomes from NAc and DLPFC. **a**) Circoplot highlights few rhythmic proteins that were identical (purple lines) and shared ontology (light blue lines) between unaffected and OUD subjects in NAc synaptosomes. Change in rhythmicity analysis in NAc Synaptosomes revealed that 0 proteins gained rhythmicity, while 23 lost rhythmicity in OUD subjects. **b**) Scatterplots of top proteins that lost rhythmicity in NAc synaptosomes between unaffected and OUD subjects. Scatterplots were generated to represent

expression rhythms for individual proteins. The x-axis represents TOD on the ZT scale and protein expression level is on y-axis, with each dot representing a subject. The red line is the fitted sinusoidal curve to reflect temporal rhythms. **c**) Pathway enrichment on proteins that changed rhythmicity between unaffected and OUD subjects in NAc synaptosomes. **d**) Circoplot highlights few rhythmic proteins that were identical (purple lines) and shared ontology (light blue lines) between unaffected and OUD subjects in DLPFC synaptosomes. Change in rhythmicity analysis in DLPFC Synaptosomes revealed that 11 proteins gained rhythmicity, while 7 lost rhythmicity. **e**) Scatterplots of top proteins that lost rhythmicity in DLPFC synaptosomes between unaffected and OUD subjects. **f**) Pathway enrichment on proteins that changed rhythmicity between unaffected and OUD subjects in DLPFC synaptosomes. Also see Figure S2 for gain/loss rhythmicity proteins in NAc and DLPFC homogenates; Supplementary Table S23 for gain/loss rhythmicity protein list in NAc homogenates; Supplementary Table S24 for gain/loss rhythmicity protein list in DLPFC homogenates; Supplementary Table S25 for gain/loss rhythmicity protein list in NAc synaptosomes; Supplementary Table S26 for gain/loss rhythmicity protein list in DLPFC synaptosomes. TOD, time of death; NAc Nucleus Accumbens; DLPFC, DorsoLateral PreFrontal Cortex.

Figure 6. Altered protein networks in NAc and DLPFC synaptosomes associated with OUD. Weight Gene Correlation Network Analysis (WGCNA) was used to generate protein coexpression modules from each brain region separately. The identified modules that survived module preservation analysis were arbitrarily assigned colors. Pie charts generated from module differential connectivity (MDC) analysis summarize modules that

gained or lost connectivity between unaffected and OUD subjects in NAc (**a**) and DLPFC (**b**). **a**) Comparing module connectivity between unaffected and OUD subjects in NAc synaptosomes identified 13 modules that lost connectivity in OUD, while 1 remained unchanged. Modules Turquoise, Green Yellow and Green were composed of several rhythmic protein hubs and showed loss in connectivity in OUD. **b**) Comparing module connectivity between unaffected and OUD subjects in DLPFC synaptosomes revealed all identified modules lost connectivity in OUD. Modules Green and Black were composed of several rhythmic hubs and showed loss of connectivity in OUD. **c**) Synaptic enrichment analysis of protein networks that lost connectivity in NAc synaptosomes. **d**) Synaptic enrichment analysis of protein networks that lost connectivity in DLPFC synaptosomes. Also see Figure S3 for WGCNA dendrograms on NAc and DLPFC homogenates; Figure S4 for WGCNA dendrograms on NAc and DLPFC synaptosomes; Figure S5 for modules from NAc homogenates; Figure S6 for modules from NAc synaptosomes; Figure S7 for modules from DLPFC homogenates; Figure S8 for modules from DLPFC synaptosomes; Figure S9 for additional MDC summaries; Supplementary Table S27 for WGCNA module assignments and proteins; Supplementary Table S28 for MDC analysis. DE, Differentially Expressed; Nucleus Accumbens; DLPFC, Dorsolateral Prefrontal Cortex.

Supplementary Material

Figure S1. Protein rhythm heatmaps. a) Heatmaps highlighting the top 200 OUD rhythmic proteins found in NAc homogenates and synaptosomes. **b**) Heatmaps highlighting that the top 200 OUD rhythmic proteins found in DLPFC homogenates and synaptosomes. Heatmaps were generated by performing supervised clustering of expression of top 200 rhythmic proteins found in homogenates from unaffected subjects and applied to OUD. Subjects were ordered by TOD to visualize expression levels over 24-hours. Yellow color indicates increased Z-score and higher protein expression, while blue color indicates decreased Z-score and lower protein expression. TOD, time of death; NAc, nucleus accumbens; DLPFC, dorsolateral prefrontal cortex.

Figure S2. Diurnal rhythms of protein expression in DLPFC and NAc homogenates associated with OUD. a) Heatmaps highlighting top 200 rhythmic proteins from NAc homogenates of unaffected subjects. Rhythmic proteins in unaffected subjects are plotted in OUD subjects to show disruption of protein rhythmicity. Heatmaps were generated by performing supervised clustering of expression of top 200 rhythmic proteins found in homogenates from Unaffected subjects and applied to OUD. Subjects were ordered by TOD to visualize expression levels over a period of 24 hours. Yellow color indicates increased Z-score and higher protein expression, while blue color indicates decreased Z-score and lower protein expression. **b**) Scatterplots of top rhythmic proteins in NAc homogenates of unaffected and OUD subjects. Scatterplots were generated to represent expression rhythms for individual proteins. The x-axis represents TOD on the ZT scale

and protein expression level is on y-axis, with each dot representing a subject. The red line is the fitted sinusoidal curve to reflect temporal rhythms. **c**) Pathway enrichment analysis of rhythmic proteins in NAc homogenates from unaffected and OUD subjects. Warmer colors indicate increasing $-\log_{10} p$ value and highly rhythmic pathways in each group. **d**) Venn diagrams showing low overlap of rhythmic proteins and genes in NAc homogenates from unaffected and OUD subjects. **e**) Heatmaps highlighting disrupted protein rhythmicity in OUD of top 200 rhythmic proteins from DLPFC homogenates of unaffected subjects. Rhythmic proteins in unaffected subjects are plotted in OUD subjects to show disruption of protein rhythmicity. **f**) Scatterplots of top rhythmic proteins in DLPFC homogenates from unaffected and OUD subjects. **g**) Pathway enrichment analysis of rhythmic proteins in DLPFC homogenates from unaffected and OUD subjects. **h**) Venn diagrams showing low overlap of rhythmic proteins in DLPFC homogenates from unaffected and OUD subjects. Also see Figure S1 for protein expression rhythm heatmaps in OUD; Supplementary Table S15 for rhythmic proteins in NAc homogenates of unaffected subjects; Supplementary Table S16 for rhythmic proteins in NAc homogenates of OUD subjects; Supplementary Table S17 for rhythmic proteins in DLPFC homogenates of unaffected subjects; Supplementary Table S18 for rhythmic proteins in DLPFC homogenates of OUD subjects. TOD, Time of Death; NAc, Nucleus Accumbens; DLPFC, Dorsolateral Prefrontal Cortex.

Figure S3. Gain/loss of protein rhythms in NAc and DLPFC homogenates. Comparison of rhythmic proteins from unaffected and OUD subjects in NAc and DLPFC

homogenates. Circoplots highlight that few rhythmic proteins were identical (purple lines) and some shared ontology (light blue lines) between the DLPFC and NAc. **a**) Change in rhythmicity analysis in NAc homogenates revealed that 19 proteins gained rhythmicity, while 5 lost rhythmicity. **b**) Change in rhythmicity analysis in DLPFC homogenates revealed that 7 proteins gained rhythmicity, while 3 lost rhythmicity. **c**) Analysis of enriched pathways in proteins changing rhythmicity between unaffected and OUD in NAc homogenates. **d**) Analysis of enriched pathways in proteins changing rhythmicity between Unaffected and OUD in DLPFC homogenates.

Figure S4. Protein networks in NAc and DLPFC homogenates. Dendrograms from WGCNA showing the average linkage hierarchical clustering of proteins. **a**) Dendrograms from NAc homogenates identified 15 and 23 modules in unaffected and OUD subjects, respectively. **b**) Dendrograms from DLPFC homogenates identified 26 and 23 modules in unaffected and OUD subjects, respectively. NAc, Nucleus Accumbens; DLPFC, Dorsolateral Prefrontal Cortex.

Figure S5. Protein networks in NAc and DLPFC synaptosomes. Dendrograms from WGCNA showing the average linkage hierarchical clustering of genes. **a**) Dendrograms from NAc Synaptosomes identified 15 and 16 modules in unaffected and OUD subjects, respectively. **b**) Dendrograms from DLPFC synaptosomes identified 11 and 09 modules in unaffected and OUD subjects, respectively. NAc, Nucleus Accumbens; DLPFC, Dorsolateral Prefrontal Cortex.

Figure S6. NAc homogenate modules. Selected networks from NAc homogenate modules of interest and significant hub enrichment of rhythmic proteins. **a**) Selected networks from base modules in unaffected to which were compared OUD. **b**) Selected networks from base modules OUD to which were compared unaffected.

Figure S7. NAc synaptosome modules. Selected networks from NAc synaptosome modules of interest and significant hub enrichment of rhythmic proteins. **a**) Selected networks from base modules in unaffected to which were compared OUD. **b**) Selected networks from base modules OUD to which were compared unaffected.

Figure S8. DLPFC homogenate modules. Selected networks from DLPFC homogenates modules of interest and significant hub enrichment of rhythmic proteins. **a**) Selected networks from base modules in unaffected to which were compared OUD. **b**) Selected networks from base modules OUD to which were compared unaffected.

Figure S9. DLPFC synaptosomes modules. Selected networks from DLPFC synaptosomes modules of interest and significant hub enrichment of rhythmic proteins. **a**) Selected networks from base modules in unaffected to which were compared OUD. **b**) Selected networks from base modules OUD to which were compared to unaffected.

Figure S10. Modulate differential connectivity of WGCNA modules.

Table S1. Subject information. Postmortem brains were collected from people diagnosed with OUD and from matched unaffected comparison subjects. Subjects were matched on age, sex, postmortem interval (PMI), brain pH, and RNA integrity (RIN). All brains were provided by the brain bank in the Department of Psychiatry at the University of Pittsburgh School of Medicine.

Table S2. Significant DE proteins in NAc homogenates. Differentially expressed proteins in tissue homogenates from NAc of subjects with OUD compared to unaffected subjects. We identified 43 DE ($p<0.05$ and logFC±0.26) proteins (14 upregulated and 29 downregulated).

Table S3. Full protein expression list in NAc homogenates. Full list of proteins detected in tissue homogenates from NAc, and levels of expression in OUD compared to unaffected subjects.

Table S4. Significant DE proteins in DLPFC homogenates. Differentially expressed proteins in tissue homogenates from DLPFC of subjects with OUD compared to unaffected subjects. We identified 55 DE proteins ($p<0.05$ and logFC±0.26), with a majority being upregulated in OUD (46 upregulated and 9 downregulated).

Table S5. Full protein expression list in DLPFC homogenates. Full list of proteins detected in tissue homogenates from DLPFC, and levels of expression in OUD compared to unaffected subjects.

Table S6. Pathway enrichment in NAc and DLPFC homogenates and synaptosomes.

Table S7. Significant DE proteins in NAc synaptosomes. Differentially expressed proteins in NAc Synaptosomes of subjects with OUD compared to unaffected subjects. We identified 56 DE proteins ($p<0.05$ and logFC±0.26), with a majority being upregulated in OUD (17 upregulated and 39 downregulated). DE, Differentially Expressed; NAc Nucleus Accumbens.

Table S8. Full protein expression list in NAc synaptosomes. Full list of proteins detected in synaptosomes from NAc and levels of expression in OUD compared to unaffected subjects.

Table S9. Significant DE proteins in DLPFC synaptosomes. Differentially expressed proteins in DLPFC synaptosomes of subjects with OUD compared to unaffected subjects. We identified 161 DE proteins ($p<0.05$ and logFC±0.26), with a majority being upregulated in OUD (80 upregulated and 81 downregulated). DE, Differentially Expressed; NAc Nucleus Accumbens.

Table S10. Full protein expression list in DLPFC synaptosomes. Full list of proteins detected in tissue synaptosomes from DLPFC and levels of expression in OUD compared to unaffected subjects.

Table S11. Protein enrichment in NAc synaptosomes.

Table S12. Protein enrichment in DLPFC synaptosomes.

Table S13. Rhythmic proteins in NAc homogenates in unaffected subjects. Analysis of rhythms (amplitude, phase, peak) in NAc homogenates from unaffected subjects, generated by plotting protein expression across time of day.

Table S14. Rhythmic proteins in NAc homogenates in OUD subjects. Analysis of rhythms (amplitude, phase, peak) in NAc homogenates from OUD subjects, generated by plotting protein expression across time of day.

Table S15. Rhythmic proteins in DLPFC homogenates in unaffected subjects. Analysis of rhythms (amplitude, phase, peak) in DLPFC homogenates from unaffected subjects, generated by plotting protein expression across time of day.

Table S16. Rhythmic proteins in DLPFC homogenates in OUD subjects. Analysis of rhythms (amplitude, phase, peak) in DLPFC homogenates from OUD subjects, generated by plotting protein expression across time of day.

Table S17. Rhythmic proteins in NAc synaptosomes in unaffected subjects. Analysis of rhythms (amplitude, phase, peak) in NAc synaptosomes from Unaffected subjects, generated by plotting protein expression across time of day.

Table S18. Rhythmic proteins in NAc synaptosomes in OUD subjects. Analysis of rhythms (amplitude, phase, peak) in NAc Synaptosomes from OUD subjects, generated by plotting protein expression across time of day.

Table S19. Rhythmic proteins in DLPFC synaptosomes in unaffected subjects. Analysis of rhythms (amplitude, phase, peak) in DLPFC synaptosomes from Unaffected subjects, generated by plotting protein expression across time of day.

Table S20. Rhythmic proteins in DLPFC synaptosomes in OUD subjects. Analysis of rhythms (amplitude, phase, peak) in DLPFC synaptosomes from OUD subjects, generated by plotting protein expression across time of day.

Table S21. Gain and loss of protein rhythms in NAc homogenates. Analysis of gain and loss of rhythms via comparison of amplitude, phase and peak of rhythmic proteins in NAc homogenates.

Table S22. Gain and loss of protein rhythms in DLPFC homogenates. Analysis of gain and loss of rhythms via comparison of amplitude, phase and peak of rhythmic proteins in DLPFC homogenates.

Table S23. Gain and loss of protein rhythms in NAc synaptosomes. Analysis of gain and loss of rhythms via comparison of amplitude, phase and peak of rhythmic proteins in NAc synaptosomes.

Table S24. Gain and loss of protein rhythms in DLPFC synaptosomes. Analysis of gain and loss of rhythms via comparison of amplitude, phase and peak of rhythmic proteins in DLPFC synaptosomes.

Table S25. WGCNA module assignments. Weight Gene Correlation Network Analysis (WGCNA) module assignment in NAc and DLPFC homogenates and synaptosomes.

Table S26. MDC analysis. Module Differential Connectivity (MDC) analysis in NAc and DLPFC homogenates and synaptosomes.

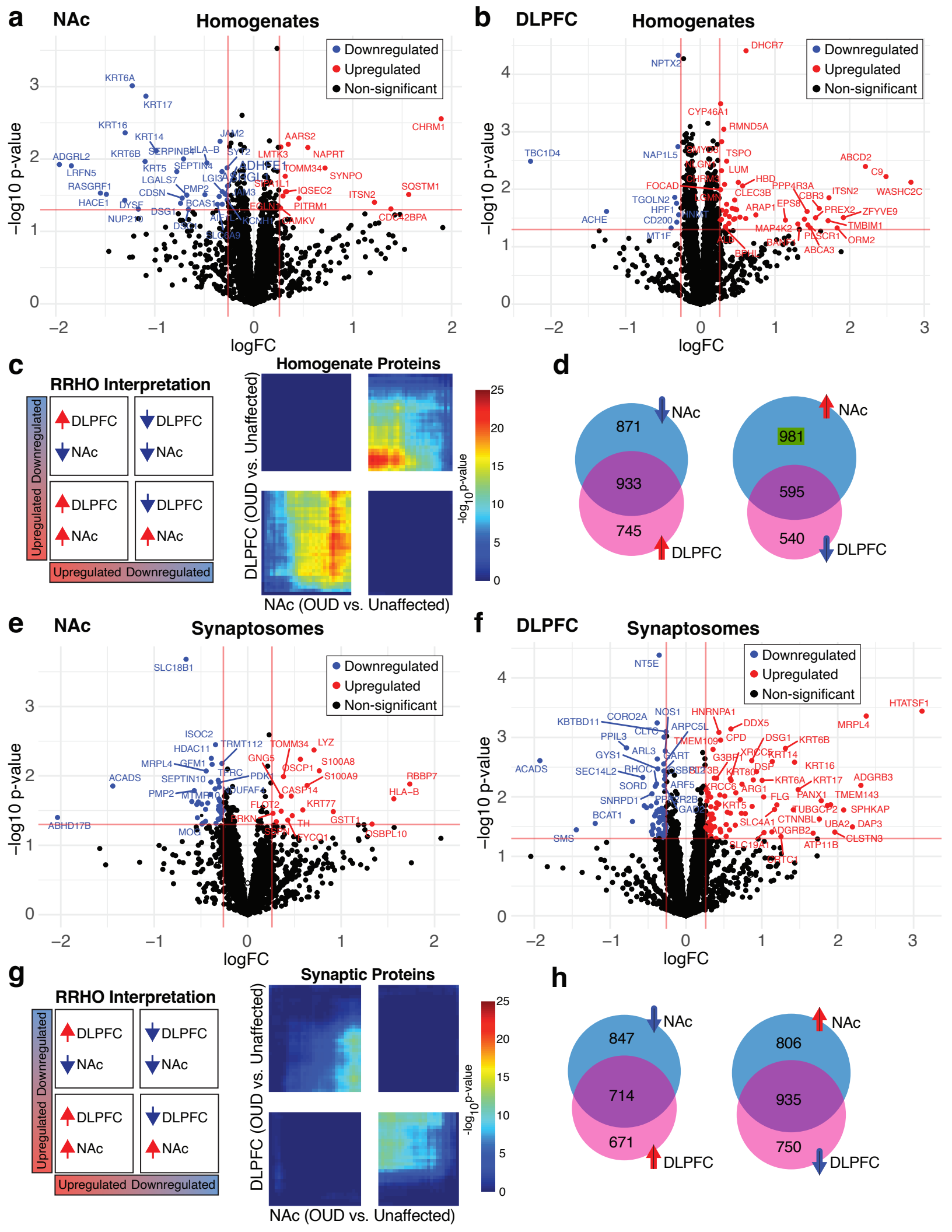
a
NAc
Homogenates
Downregulated
Upregulated
Non-significant
−log10 p-value
logFC
KRT6A
KRT17
KRT16
KRT14
KRT6B
SERPINB4
HLA-B
ADGRL2
LRFN5
KRT5
SEPTIN4
RASGRF1
LGALS7
LGI3
CDSN
PMP2
HACE1
DYSF
BCAS1
DSG1
NUP210
JAM2
SYT2
ADHFE1
ASGL1
JAM3
EGLN3
PITRM1
KCNH7
CAMKV
SLC6A9
AARS2
LMTK3
NAPRT
TOMM34
SYNPO
SPA1L1
IQSEC2
ITSN2
SQSTM1
CDC42BPA
CHRM1
b
DLPFC
Homogenates
DHCR7
NPTX2
CYP46A1
RMND5A
TBC1D4
NAP1L5
TSPO
LUM
ABCD2
C9
WASHC2C
FOCAD
HBD
CLEC3B
PPP4R3A
ITSN2
CBR3
TGOLN2
HPF1
CD200
ACHE
MT1F
ARAP1
EPS8
PREX2
ZFYVE9
TMBIM1
MAP4K2
PLSCR1
ORM2
ABCA3
c
RRHO Interpretation
Upregulated Downregulated
DLPFC
NAc
Homogenate Proteins
DLPFC (OUD vs. Unaffected)
NAc (OUD vs. Unaffected)
-log10 p-value
d
NAc
871
933
745
DLPFC
NAc
981
595
540
DLPFC
e
NAc
Synaptosomes
Downregulated
Upregulated
Non-significant
−log10 p-value
logFC
SLC18B1
ISOC2
HDAC11
TRMT112
TOMM34
LYZ
MRPL4
GEM1
GNG5
S100A8
ACADS
SEPTIN10
PDK1
OSCP1
S100A9
RBBP7
PMP2
CASP14
HLA-B
FLOT2
KRT77
ABHD17B
GSTT1
TH
FYCO1
OSBPL10
f
DLPFC
Synaptosomes
Downregulated
Upregulated
Non-significant
−log10 p-value
logFC
NT5E
HTATSF1
NOS1
HNRNPA1
KBTBD11
CORO2A
ARPC5L
DDX5
MRPL4
CLTC
PPIL3
TMEM109
CPD
DSG1
KRT6B
GYS1
ARL3
GART
G3BP1
KRT14
ACADS
SEC14L2
RHOC
DSP
KRT16
SORD
ARF5
KRT80
KRT6A
KRT17
ADGRB3
SNRPD1
KRCC6
ARG1
FLG
PANX1
TMEM143
BCAT1
KRT15
TUBGCP2
SPHKAP
SLC4A1
CTNNBL1
UBA2
DAP3
SMS
ADGRB2
CLSTN3
ATP11B
g
RRHO Interpretation
Upregulated Downregulated
DLPFC
NAc
Synaptic Proteins
DLPFC (OUD vs. Unaffected)
NAc (OUD vs. Unaffected)
-log10 p-value
h
NAc
847
714
671
DLPFC
NAc
806
935
750
DLPFC

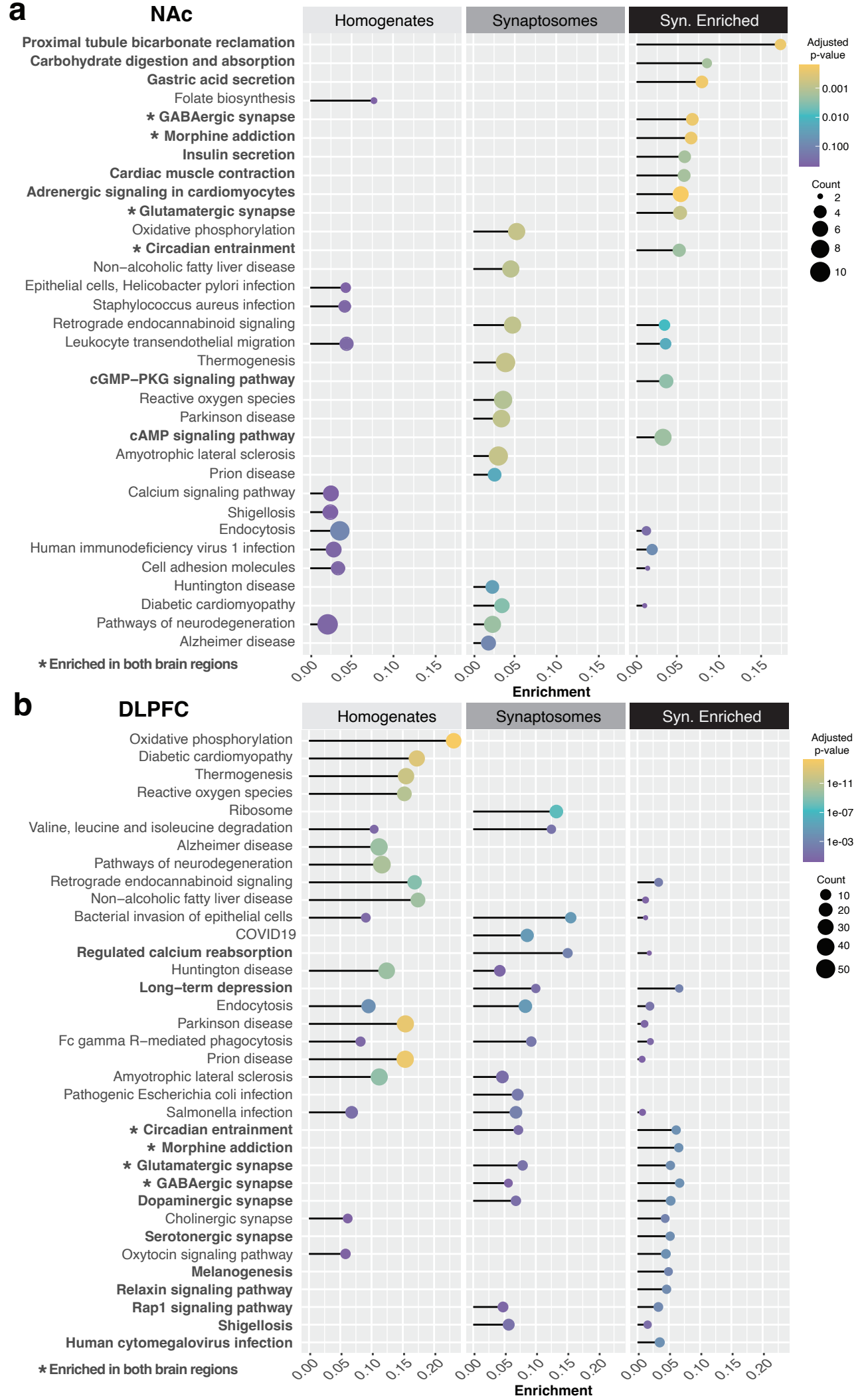
a
NAc
Homogenates
Synaptosomes
Syn. Enriched
Proximal tubule bicarbonate reclamation
Carbohydrate digestion and absorption
Gastric acid secretion
Folate biosynthesis
* GABAergic synapse
* Morphine addiction
Insulin secretion
Cardiac muscle contraction
Adrenergic signaling in cardiomyocytes
* Glutamatergic synapse
Oxidative phosphorylation
* Circadian entrainment
Non−alcoholic fatty liver disease
Epithelial cells, Helicobacter pylori infection
Staphylococcus aureus infection
Retrograde endocannabinoid signaling
Leukocyte transendothelial migration
Thermogenesis
cGMP−PKG signaling pathway
Reactive oxygen species
Parkinson disease
cAMP signaling pathway
Amyotrophic lateral sclerosis
Prion disease
Calcium signaling pathway
Shigellosis
Endocytosis
Human immunodeficiency virus 1 infection
Cell adhesion molecules
Huntington disease
Diabetic cardiomyopathy
Pathways of neurodegeneration
Alzheimer disease
* Enriched in both brain regions
0.00 0.05 0.10 0.15
Enrichment
Adjusted p-value
0.001
0.010
0.100
Count
2
4
6
8
10
b
DLPFC
Homogenates
Synaptosomes
Syn. Enriched
Oxidative phosphorylation
Diabetic cardiomyopathy
Thermogenesis
Reactive oxygen species
Ribosome
Valine, leucine and isoleucine degradation
Alzheimer disease
Pathways of neurodegeneration
Retrograde endocannabinoid signaling
Non−alcoholic fatty liver disease
Bacterial invasion of epithelial cells
COVID19
Regulated calcium reabsorption
Huntington disease
Long−term depression
Endocytosis
Parkinson disease
Fc gamma R−mediated phagocytosis
Prion disease
Amyotrophic lateral sclerosis
Pathogenic Escherichia coli infection
Salmonella infection
* Circadian entrainment
* Morphine addiction
* Glutamatergic synapse
* GABAergic synapse
Dopaminergic synapse
Cholinergic synapse
Serotonergic synapse
Oxytocin signaling pathway
Melanogenesis
Relaxin signaling pathway
Rap1 signaling pathway
Shigellosis
Human cytomegalovirus infection
* Enriched in both brain regions
0.00 0.05 0.10 0.15 0.20
Enrichment
Adjusted p-value
1e-11
1e-07
1e-03
Count
10
20
30
40
50

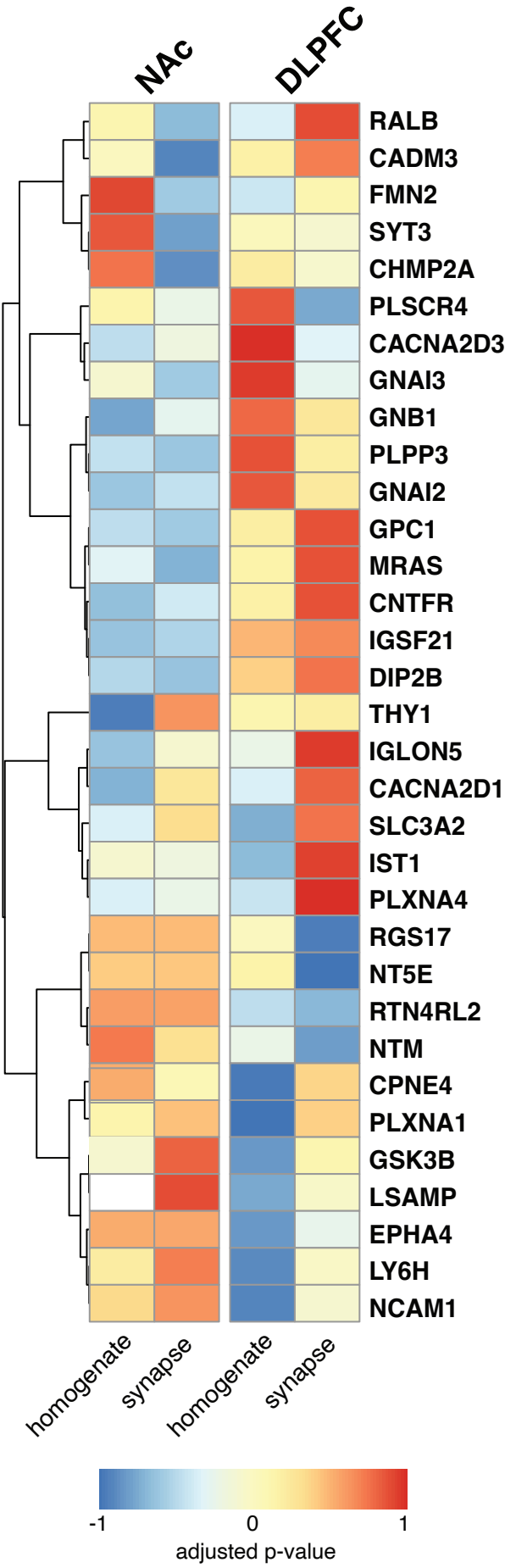
Proteins Altered in OUD and Enriched in Synaptosomes
NAc
DLPFC
RALB
CADM3
FMN2
SYT3
CHMP2A
PLSCR4
CACNA2D3
GNAI3
GNB1
PLPP3
GNAI2
GPC1
MRAS
CNTFR
IGSF21
DIP2B
THY1
IGLON5
CACNA2D1
SLC3A2
IST1
PLXNA4
RGS17
NT5E
RTN4RL2
NTM
CPNE4
PLXNA1
GSK3B
LSAMP
EPHA4
LY6H
NCAM1
homogenate
synapse
homogenate
synapse
-1
0
1
adjusted p-value

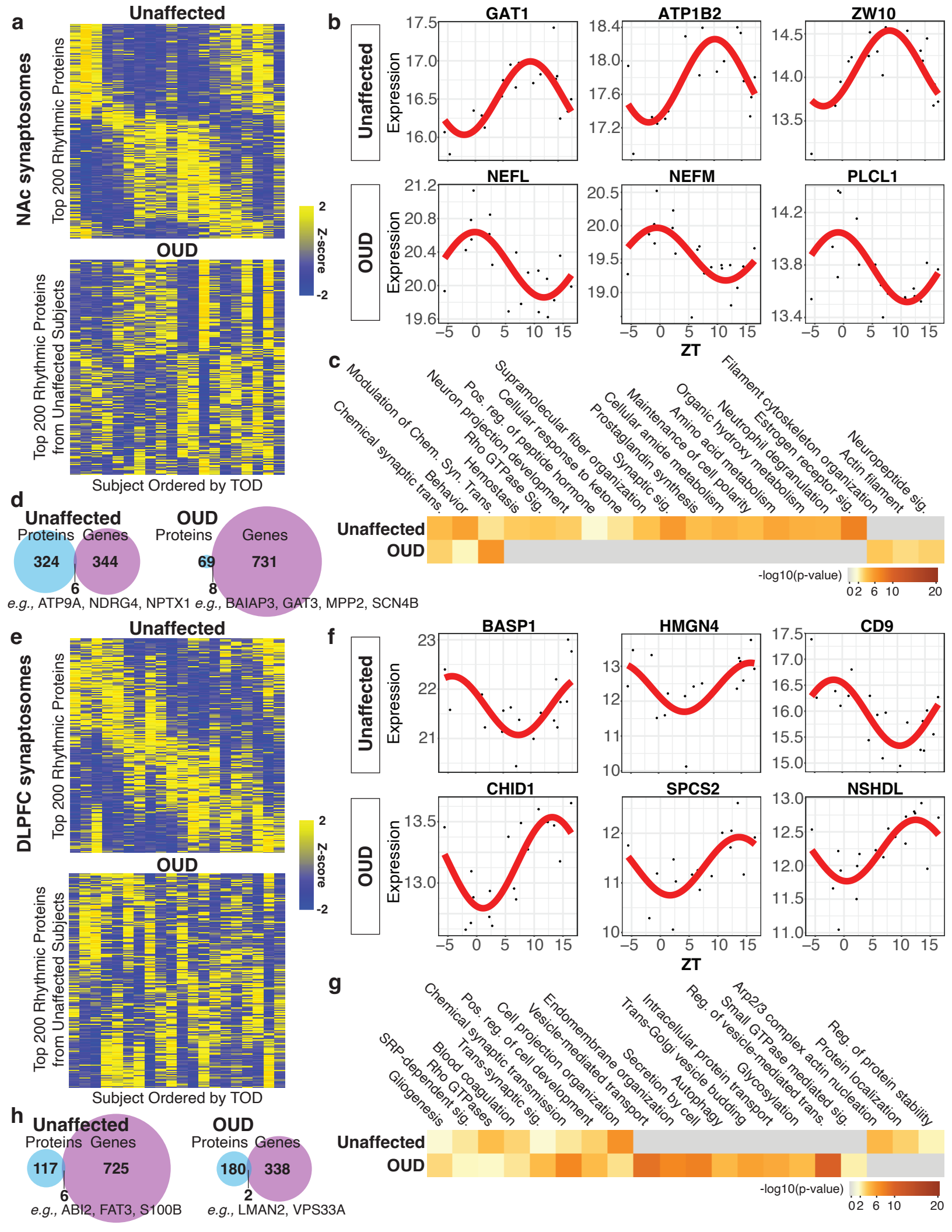
a
NAc synaptosomes
Unaffected
Top 200 Rhythmic Proteins
OUD
Top 200 Rhythmic Proteins from Unaffected Subjects
Subject Ordered by TOD
Z-score
2
-2
b
Unaffected
OUD
Expression
GAT1
ATP1B2
ZW10
NEFL
NEFM
PLCL1
ZT
c
Modulation of Chem. Syn. Trans.
Chemical synaptic trans.
Behavior
Hemostasis
Rho GTPase Sig.
Neuron projection development
Pos. reg. of peptide hormone
Cellular response to ketone
Supramolecular fiber organization
Prostaglandin synthesis
Synaptic sig.
Cellular amide metabolism
Maintenance of cell polarity
Amino acid metabolism
Organic hydroxy metabolism
Neutrophil degranulation
Estrogen receptor sig.
Filament cytoskeleton organization
Actin filament
Neuropeptide sig.
Unaffected
OUD
-log10(p-value)
d
Unaffected
Proteins
Genes
324
344
6
e.g., ATP9A, NDRG4, NPTX1
OUD
Proteins
Genes
69
731
8
e.g., BAIAP3, GAT3, MPP2, SCN4B
e
DLPFC synaptosomes
Unaffected
Top 200 Rhythmic Proteins
OUD
Top 200 Rhythmic Proteins from Unaffected Subjects
Subject Ordered by TOD
Z-score
2
-2
f
Unaffected
OUD
Expression
BASP1
HMGN4
CD9
CHID1
SPCS2
NSHDL
ZT
g
SRP-dependent sig.
Gliogenesis
Blood coagulation
Rho GTPases
Trans-synaptic sig.
Chemical synaptic transmission
Pos. reg. of cell development
Cell projection organization
Vesicle-mediated transport
Endomembrane organization
Secretion by cell
Trans-Golgi vesicle budding
Autophagy
Intracellular protein transport
Glycosylation
Reg. of vesicle-mediated trans.
Small GTPase mediated sig.
Arp2/3 complex actin nucleation
Protein localization
Reg. of protein stability
Unaffected
OUD
-log10(p-value)
h
Unaffected
Proteins
Genes
117
725
6
e.g., ABI2, FAT3, S100B
OUD
Proteins
Genes
180
338
2
e.g., LMAN2, VPS33A

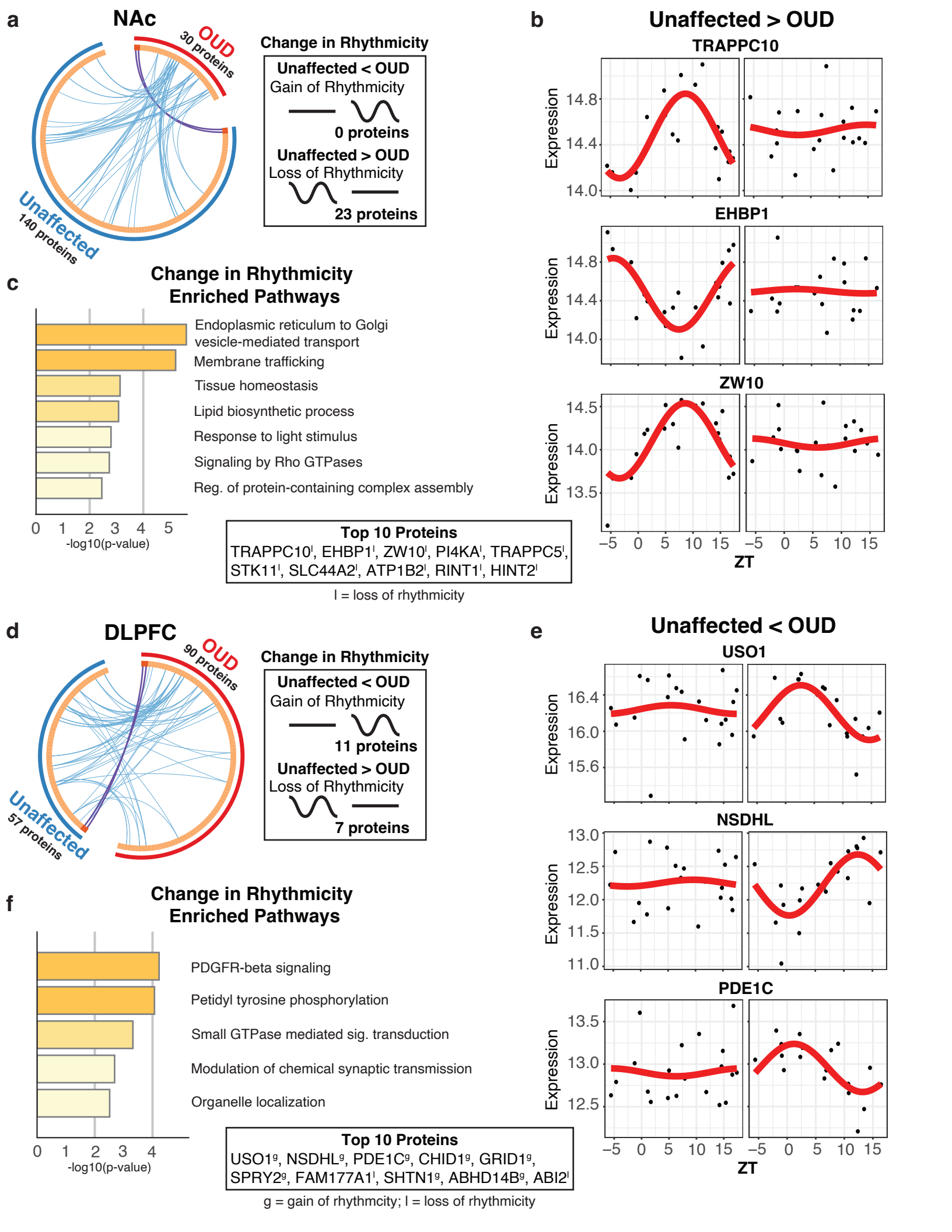
a
NAc
OUD
30 proteins
Unaffected
140 proteins
Change in Rhythmicity
Unaffected < OUD
Gain of Rhythmicity
0 proteins
Unaffected > OUD
Loss of Rhythmicity
23 proteins
b
Unaffected > OUD
TRAPPC10
EHBP1
ZW10
Expression
ZT
c
Change in Rhythmicity
Enriched Pathways
Endoplasmic reticulum to Golgi vesicle-mediated transport
Membrane trafficking
Tissue homeostasis
Lipid biosynthetic process
Response to light stimulus
Signaling by Rho GTPases
Reg. of protein-containing complex assembly
-log10(p-value)
Top 10 Proteins
TRAPPC10[l], EHBP1[l], ZW10[l], PI4KA[l], TRAPPC5[l], STK11[l], SLC44A2[l], ATP1B2[l], RINT1[l], HINT2[l]
l = loss of rhythmicity
d
DLPFC
OUD
90 proteins
Unaffected
57 proteins
Change in Rhythmicity
Unaffected < OUD
Gain of Rhythmicity
11 proteins
Unaffected > OUD
Loss of Rhythmicity
7 proteins
e
Unaffected < OUD
USO1
NSDHL
PDE1C
Expression
ZT
f
Change in Rhythmicity
Enriched Pathways
PDGFR-beta signaling
Petidyl tyrosine phosphorylation
Small GTPase mediated sig. transduction
Modulation of chemical synaptic transmission
Organelle localization
-log10(p-value)
Top 10 Proteins
USO1[g], NSDHL[g], PDE1C[g], CHID1[g], GRID1[g], SPRY2[g], FAM177A1[l], SHTN1[g], ABHD14B[g], ABI2[l]
g = gain of rhythmcity; l = loss of rhythmicity

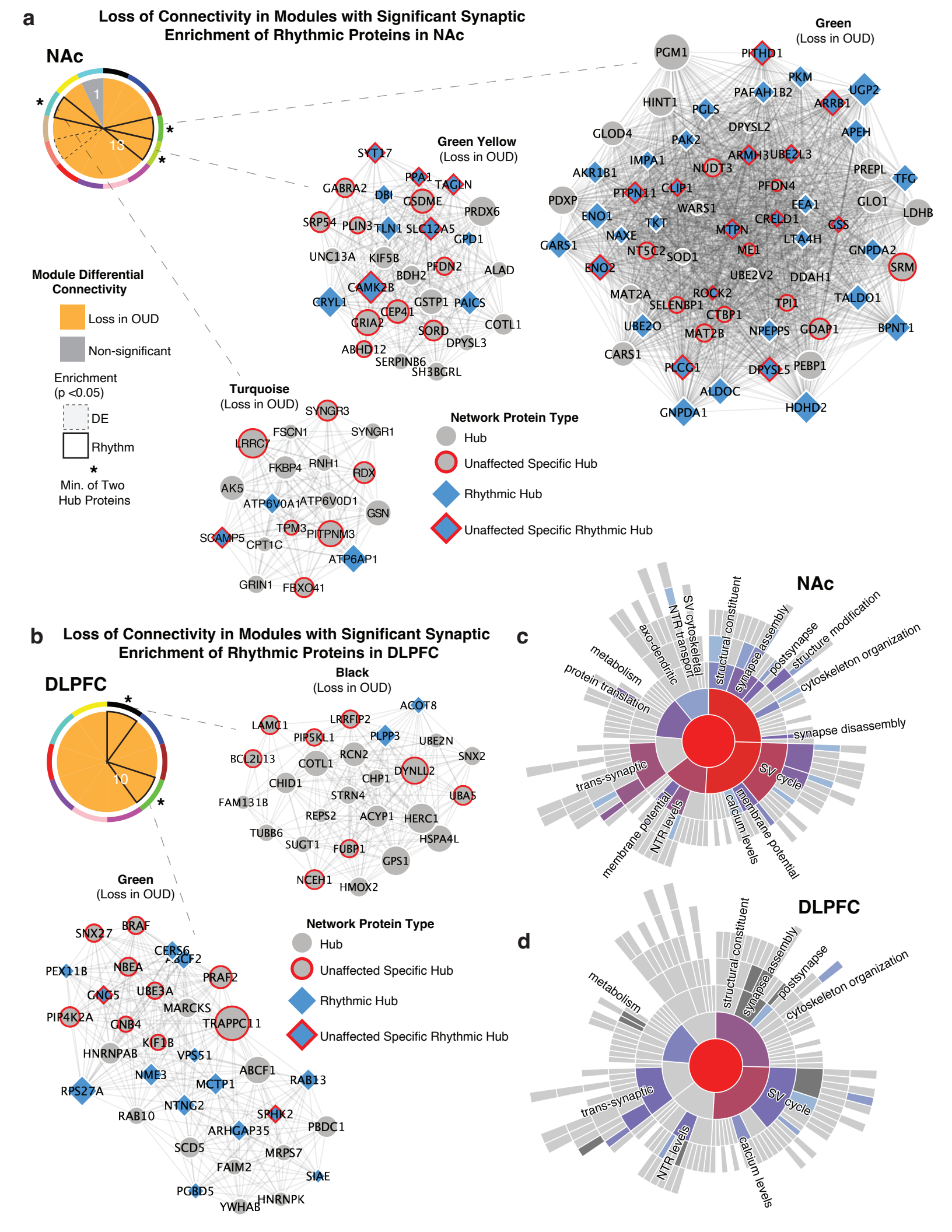
a
Loss of Connectivity in Modules with Significant Synaptic Enrichment of Rhythmic Proteins in NAc
NAc
1
13
Green
(Loss in OUD)
PGM1
PKTHD1
PKM
PAFAH1B2
UGP2
ARRB1
HINT1
PGLS
DPYSL2
APEH
GLOD4
PAK2
ARMH3
UBE2L3
IMPA1
NUDT3
PREPL
AKR1B1
TFG
PTPN11
CLIP1
PFDN4
PDXP
WARS1
EEA1
GLO1
ENO1
TKT
CRELD1
GSS
LDHB
NAXE
MTPN
LTA4H
GARS1
NT5C2
SOD1
ME1
GNPDA2
ENO2
UBE2V2
DDAH1
SRM
MAT2A
ROCK2
TALDO1
SELENBP1
TPI1
CTBP1
UBE2O
MAT2B
NPEPPS
GDAP1
BPNT1
CARS1
PLCG1
DPYSL5
PEBP1
ALDOC
GNPDA1
HDHD2
Green Yellow
(Loss in OUD)
SYT17
PPA1
TAGLN
GABRA2
DBI
GSDME
PRDX6
SRP54
PLIN3
TLN1
SLC12A5
GPD1
UNC13A
KIF5B
PFDN2
ALAD
BDH2
CAMK2B
CRYL1
GSTP1
PAICS
CEP41
GRIA2
COTL1
SORD
DPYSL3
ABHD12
SERPINB6
SH3BGRL
Module Differential Connectivity
Loss in OUD
Non-significant
Enrichment
(p <0.05)
DE
Rhythm
*
Min. of Two
Hub Proteins
Turquoise
(Loss in OUD)
SYNGR3
FSCN1
SYNGR1
LRRC7
FKBP4
RNH1
RDX
AK5
ATP6V0A1
ATP6V0D1
GSN
TPM3
PITPNM3
SGAMP5
CPT1C
ATP6AP1
GRIN1
FBXO41
Network Protein Type
Hub
Unaffected Specific Hub
Rhythmic Hub
Unaffected Specific Rhythmic Hub
b
Loss of Connectivity in Modules with Significant Synaptic Enrichment of Rhythmic Proteins in DLPFC
DLPFC
10
Black
(Loss in OUD)
ACOT8
LAMC1
LRRFIP2
PIP5KL1
PLPP3
UBE2N
BCL2L13
COTL1
RCN2
SNX2
CHID1
CHP1
DYNLL2
STRN4
UBA5
FAM131B
REPS2
ACYP1
HERC1
TUBB6
HSPA4L
SUGT1
FUBP1
GPS1
NCEH1
HMOX2
Green
(Loss in OUD)
SNX27
BRAF
CERS6
ABCF2
PEX11B
NBEA
PRAF2
GNG5
UBE3A
MARCKS
PIP4K2A
GNB4
TRAPPC11
KIF1B
HNRNPAB
VPS51
NME3
ABCF1
RAB13
RPS27A
MCTP1
NTNG2
RAB10
SPHK2
ARHGAP35
PBDC1
SCD5
MRPS7
FAIM2
SIAE
PGBD5
YWHAB
HNRNPK
Network Protein Type
Hub
Unaffected Specific Hub
Rhythmic Hub
Unaffected Specific Rhythmic Hub
c
NAc
SV cytoskeletal
NTR transport
structural constituent
synapse assembly
postsynapse
structure modification
cytoskeleton organization
axo-dendritic
metabolism
protein translation
synapse disassembly
trans-synaptic
SV cycle
membrane potential
NTR levels
calcium levels
membrane potential
d
DLPFC
structural constituent
synapse assembly
postsynapse
cytoskeleton organization
metabolism
trans-synaptic
SV cycle
NTR levels
calcium levels